Deep water temperature, carbonate ion, and ice volume changes across the Eocene-Oligocene climate transition

A. E. Pusz,[1] R. C. Thunell,[1] and K. G. Miller[2]

[1] Paired benthic foraminiferal stable isotope and Mg/Ca data are used to estimate bottom water temperature (BWT) and ice volume changes associated with the Eocene-Oligocene Transition (EOT), the largest global climate event of the past 50 Myr. We utilized ODP Sites 1090 and 1265 in the South Atlantic to assess seawater $\delta^{18}O$ (δ_w), Antarctic ice volume, and sea level changes across the EOT (~33.8–33.54 Ma). We also use benthic $\delta^{13}C$ data to reconstruct the sources of the deep water masses in this region during the EOT. Our data, together with previously published records, indicate that a pulse of Northern Component Water influenced the South Atlantic immediately prior to and following the EOT. Benthic $\delta^{18}O$ records show a 0.5‰ increase at ~33.8 Ma (EOT-1) that represents a ~2°C cooling and a small (~10 m) eustatic fall that is followed by a 1.0‰ increase associated with Oi-1. The expected cooling of deep waters at Oi-1 (~33.54 Ma) is not apparent in our Mg/Ca records. We suggest the cooling is masked by coeval changes in the carbonate saturation state ($\Delta[CO_3^{2-}]$) which affect the Mg/Ca data. To account for this, the BWT, ice volume, and δ_w estimates are corrected for a change in the $\Delta[CO_3^{2-}]$ of deep waters on the basis of recently published work. Corrected BWT at Sites 1090 and 1265 show a ~1.5°C cooling coincident with Oi-1 and an average δ_w increase of ~0.75‰. The increase in ice volume during Oi-1 resulted in a ~70 m drop in global sea level and the development of an Antarctic ice sheet that was near modern size or slightly larger.

1. Introduction

[2] Earth's climate has experienced a long-term cooling over the past 50 million years as evidenced by a 5‰ increase in deep sea benthic foraminiferal $\delta^{18}O$ during this period [*Savin et al.*, 1975; *Shackleton and Kennett*, 1975; *Miller et al.*, 1987, 2005; *Zachos et al.*, 2001]. Resultant oxygen isotope temperature estimates [*Miller et al.*, 1987, 2005; *Zachos et al.*, 2001], along with benthic foraminiferal Mg/Ca paleotemperatures, suggest as much as a ~12°C cooling of deep waters over the past 50 Myr [*Lear et al.*, 2000; *Billups and Schrag*, 2002, 2003]. The Cenozoic cooling trend has been attributed to changes in ocean-atmosphere circulation patterns associated with opening and closing of ocean gateways [*Kennett*, 1977; *Schnitker*, 1980; *Woodruff and Savin*, 1989; *Wright et al.*, 1992; *Raymo*, 1994] and changes in atmospheric CO_2 levels [*Vincent and Berger*, 1985; *Flower and Kennett*, 1993; *DeConto and Pollard*, 2003; *Pagani et al.*, 2005; *Pearson et al.*, 2009].

[3] The Eocene-Oligocene transition (EOT) was the largest of several abrupt events that punctuated the overall Cenozoic cooling trend [*Berger*, 1982; *Miller et al.*, 1987; *Zachos et al.*, 2001]. In well-resolved records, the ~1.5‰ benthic foraminiferal $\delta^{18}O$ increase at the EOT appears to be a two-step event with the first phase beginning at 33.8 Ma (0.5‰) followed by a second increase of 1.0‰, Oi-1 ("Oligocene isotope event 1"), at 33.54 Ma [*Miller et al.*, 1991, 2008; *Zachos et al.*, 1996; *Coxall et al.*, 2005]. The $\delta^{18}O$ shift across the EOT reflects both deep water cooling and the development of continental-size ice sheets on Antarctica [*Miller et al.*, 1991, 2005; *Zachos et al.*, 1996; *Coxall et al.*, 2005; *Lear et al.*, 2008]. Independent evidence for the onset of Antarctic glaciation associated with the EOT includes the presence of ice rafted detritus at high southern latitudes and changes in clay mineralogy in the Southern Ocean [*Ehrmann*, 1991; *Ehrmann and Mackensen*, 1992; *Zachos et al.*, 1992; *Robert et al.*, 2002].

[4] Mg/Ca ratios of benthic foraminiferal calcite can serve as an independent proxy for bottom water temperature [*Nurnberg et al.*, 1996; *Rosenthal et al.*, 1997; *Lea et al.*, 1999; *Elderfield and Ganssen*, 2000]. However, the primary BWT component can be masked by changes in the carbonate ion concentration ($[CO_3^{2-}]$) and saturation state ($\Delta[CO_3^{2-}]$) of deep waters [*Elderfield et al.*, 2006; *Rosenthal et al.*, 2006; *Yu and Elderfield*, 2008]. The $[CO_3^{2-}]$ ion effect is based on core top Mg/Ca calibrations that show

[1]Department of Earth and Ocean Sciences, University of South Carolina, Columbia, South Carolina, USA.
[2]Department of Earth and Planetary Sciences, Rutgers University, Piscataway, New Jersey, USA.
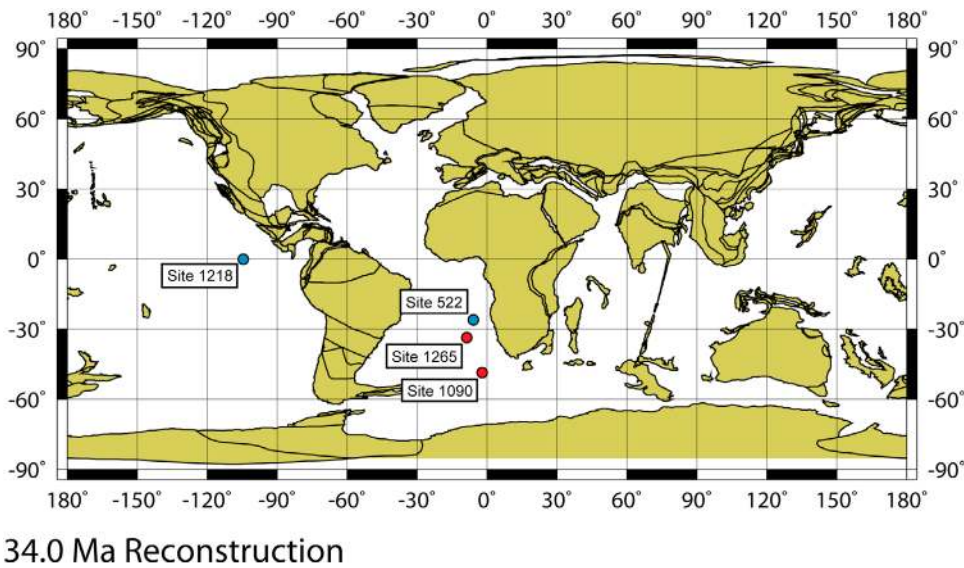
Figure 1. Paleogeographic reconstruction for 34 Ma showing the locations of Ocean Drilling Program (ODP) Sites 1090 and 1265 used in this study (red circles) and Deep Sea Drilling Project (DSDP) Site 522 and ODP Site 1218 (blue circles) from previous studies [*Zachos et al.*, 1996; *Coxall et al.*, 2005]. The map was created using the Ocean Drilling Stratigraphic Network (http://www.odsn.de/).

higher temperature sensitivities in waters <3°C [*Martin et al.*, 2002] attributed to the $[CO_3^{2-}]$ and $\Delta[CO_3^{2-}]$ of seawater [*Elderfield et al.*, 2006; *Rosenthal et al.*, 2006; *Healey et al.*, 2008; *Yu and Elderfield*, 2008]. A change in the $[CO_3^{2-}]$ is important since there is a large-scale (>1 km) drop in the carbonate compensation depth (CCD) associated with the EOT [*van Andel*, 1975; *Coxall et al.*, 2005]. Thus, paired benthic foraminiferal $\delta^{18}O$ and Mg/Ca ratios that are corrected for a change in the $[CO_3^{2-}]$ of deep waters can, in principle, be used to differentiate the contributions of ice volume and temperature to the $\delta^{18}O$ increase at the EOT.

[5] Initial Mg/Ca studies of the past 50 million years at a low resolution indicated there was no major change in BWT across the EOT [*Lear et al.*, 2000; *Billups and Schrag*, 2003], implying that the entire 1.5‰ $\delta^{18}O$ increase was due to an ice volume change. Subsequent work at a higher resolution by *Lear et al.* [2004] using South Atlantic Deep Sea Drilling Project (DSDP) Site 522 and equatorial Pacific Ocean Drilling Program (ODP) Site 1218 inferred a ~2°C warming of deep water associated with Oi-1 (Figure 1). However, any increase in BWT poses a problem because it requires more growth of ice than can be accommodated on Antarctica today [*Coxall et al.*, 2005; *DeConto et al.*, 2008]. The issue of ice accommodation space led to the hypothesis that there were significant Northern Hemisphere ice sheets during the earliest Oligocene [*Coxall et al.*, 2005; *Tripati et al.*, 2005]. No definitive evidence of large-scale Eocene-Oligocene northern hemisphere glaciation exists, leaving only the current hypothesis of small valley glaciers and ephemeral ice caps to explain the presence of drop stones recently identified off the coast of Greenland [*Eldrett et al.*, 2007].

[6] A more likely scenario points toward a change in the $\Delta[CO_3^{2-}]$ of deep waters caused by a global CCD drop that influenced benthic foraminiferal Mg/Ca ratios across the EOT [*van Andel*, 1975; *Lear et al.*, 2004; *Coxall et al.*, 2005; *Rea and Lyle*, 2005]. Benthic foraminiferal Li/Ca ratios support the hypothesis that an increased $[CO_3^{2-}]$ of deep waters is the primary influence on benthic foraminiferal Mg/Ca records across the EOT [*Lear and Rosenthal*, 2006; *Lear et al.*, 2010; *Peck et al.*, 2010]. Benthic foraminiferal Li/Ca ratios provide a way to estimate a change in deep water $[CO_3^{2-}]$ because of a response to calcification rates that is influenced by the seawater $[CO_3^{2-}]$ [*Hall and Chan*, 2004; *Lear and Rosenthal*, 2006].

[7] A recent study estimated a ~29 μmol/kg $[CO_3^{2-}]$ increase in South Atlantic deep waters coincident with Oi-1 based on benthic foraminiferal Li/Ca ratios [*Peck et al.*, 2010]. Similarly, it is reported that there was a ~37 μmol/kg $[CO_3^{2-}]$ rise in equatorial Pacific deep waters associated with Oi-1 [*Lear and Rosenthal*, 2006; *Lear et al.*, 2010]. We use published Li/Ca records from ODP Site 1263 on the Walvis Ridge [*Peck et al.*, 2010] and ODP Site 1218 in the equatorial Pacific [*Lear et al.*, 2010] to correct for benthic foraminiferal Mg/Ca overprinting due to $[CO_3^{2-}]$ changes associated with Oi-1. Site 1218 Li/Ca data [*Lear et al.*, 2010] was selected to correct our Site 1090 benthic foraminiferal Mg/Ca record because of its paleowater depth (≥3.7 km at ~34 Ma). The Site 1263 Li/Ca record [*Peck et al.*, 2010] was chosen to correct Site 1265 Mg/Ca ratios because it is in close proximity and has a similar paleowater depth at ~34 Ma. The $[CO_3^{2-}]$ correction factor used on our benthic foraminiferal Mg/Ca data is based on an empirical sensitivity of 0.0086 mmol/mol/μmol/kg [*Elderfield et al.*, 2006].

[8] Two deep sea sediment records with complete sections across the EOT are utilized in the present study to investigate deep water temperature and global ice volume changes. We chose South Atlantic ODP Sites 1090 and 1265 (Figure 1) because of excellent core recovery, high carbonate content, and good foraminiferal preservation. Orbital-scale resolution (10 and 40 cm sampling) benthic foraminiferal (*Cibicidoides* spp.) $\delta^{18}O$, $\delta^{13}C$, and Mg/Ca records were generated across

the EOT for both sites. As mentioned above, Sites 1090 and 1265 benthic foraminiferal Mg/Ca records are corrected for changes in the $[CO_3^{2-}]$ based on recent Li/Ca data from *Peck et al.* [2010] and *Lear et al.* [2010].

[9] We assess the reliability of our benthic foraminiferal stable isotope records by placing them into a global context using the multisite isotopic compilation from *Cramer et al.* [2009]. Benthic foraminiferal $\delta^{13}C$ data across the EOT from South Atlantic Sites 1090 and 1265 are compared to existing records from equatorial Pacific ODP Site 1218 [*Coxall et al.*, 2005] and South Atlantic DSDP Site 522 [*Zachos et al.*, 1996] to reconstruct source regions for deep water masses (Figure 1). Previous stable isotope work at Site 1265 [*Liu et al.*, 2004] reported on the benthic foraminiferal species *C. praemundulus* at a low resolution (~50 kyr) from two separate holes across the EOT. Site 1265 stable isotope and trace metal data from the present study is derived from a single hole (1265B) at a higher resolution (10 cm; equivalent to ~17 kyr) in efforts to gain complete coverage of changes in deep water across the EOT.

2. Methods

2.1. Site Selection and Age Control

[10] South Atlantic ODP Site 1090 hole B is located on the southern flank of the Agulhas Ridge (42°54.8′S, 8°53.9′E) at a water depth of 3702 m, which is above the present-day lysocline depth (4300 m) [*Milliman*, 1993; *Dittert and Henrich*, 2000]. The paleowater depth for Site 1090 is estimated to have been ~3000–3300 m at ~34 Ma (using equations of *Miller et al.* [1986] and *Stein and Stein* [1992] and the following parameters: present water depth of 3702 m, sediment thickness of 800 m, basement age of 87 Ma, and preexponential empirical constant of −3650). The CCD at ~34 Ma was positioned at ~3100 m in the South Atlantic [*Peck et al.*, 2010]. Site 1090 was located at approximately 49°S, 2°E at ~34 Ma [*Anderson and Delaney*, 2005]. The Eocene-Oligocene boundary interval is located in sediments classified as nannofossil-diatom ooze with approximately 30 weight percent carbonate [*Gersonde et al.*, 1999]. A total of one hundred and eighteen samples were taken at 40 cm intervals between 35 and 33.1 Ma (225–287 mcd), representing a sample spacing of ~10 kyr. ODP Site 1090 has excellent age control (Figures S1 and S2 in the auxiliary material) based on previously published magnetostratigraphy that is correlated to the geomagnetic polarity time scale (GPTS) [*Channell et al.*, 2003].[1] Average sedimentation rates for the latest Eocene to earliest Oligocene section at Site 1090 are ~3.7 cm/kyr.

[11] South Atlantic ODP Site 1265 hole B is located on the Walvis Ridge (28°50.1′S, 2°38.3′E) at 3083 m water depth [*Zachos et al.*, 2004]. The present-day position of the lysocline in the Cape Basin is 4000 m [*Hodell et al.*, 2001; *Volbers and Henrich*, 2002; *Henrich et al.*, 2003]. The paleowater depth for Site 1265 at ~34 Ma was ~2400 m [*Zachos et al.*, 2004] and the CCD was at ~3100 m [*Peck et al.*, 2010]. The paleolatitude for Site 1265 was ~34°S, 9°E during the latest Eocene [http://www.odsn.de/]. The

EOT sediments at this location display a change in composition from uppermost Eocene clay bearing nannofossil ooze to lowermost Oligocene foraminiferal-dominated nannofossil ooze with carbonate content between 85% and 95% [*Zachos et al.*, 2004]. A total of 121 samples were taken every 10 cm (equivalent to ~17 kyr) between 32.8 and 34.2 Ma (183–196 mcd). Age control for Site 1265 is based on the age-depth model determined from magnetostratigraphy and calcareous nannofossil stratigraphy [*Zachos et al.*, 2004]. Sedimentation rates for the latest Eocene to earliest Oligocene interval average ~0.5 cm/kyr.

[12] The foraminiferal tests used are from burial depths of 180–200 m for Site 1265 and 200–300 m for Site 1090 and thus may have undergone some postdepositional dissolution of the primary calcite [*Liu et al.*, 2004]. Postburial dissolution can alter the Mg/Ca ratios of foraminiferal tests by preferentially removing Mg-rich calcite causing artificially colder temperatures [e.g., *Brown and Elderfield*, 1996; *Dekens et al.*, 2002; *Regenberg et al.*, 2006; *Rosenthal and Lohmann*, 2002; *Rosenthal et al.*, 2000]. Similarly, postburial accumulation of secondary calcite can modify the primary Mg/Ca ratio and yield spuriously colder temperatures estimates depending on the amount and composition of recrystallization [*Baker et al.*, 1982; *Delaney*, 1989]. Scanning electron microscope (SEM) images of benthic foraminiferal tests from Sites 1090 and 1265 reveal excellent preservation, with no indication of secondary calcification (Figure 2). Furthermore, any potential BWT change resulting from minor dissolution/diagenesis would be less than the analytical (±0.9°C) or calibration (±1.3°C) error; major diagenesis is precluded based on the excellent preservation revealed by SEM micrographs. We conclude the original isotopic and geochemical signals incorporated in the foraminiferal tests are not altered by diagenesis or dissolution based on our SEM images for both sites (Figure 2).

[13] Oxygen and carbon isotope data for Sites 1090 and 1265 are plotted versus depth, core recovery, magneto-chronology, biostratigraphic zones, and lithology to estimate sedimentation rates and develop age models (Figures S1 and S2 in the auxiliary material). Though both sites lack a precise orbital chronology, intersite correlations suggest that the magnetobiostratigraphic age models (Figure 3) have uncertainties of less than 0.1 Myr. Chronology for Site 1090 relies primarily on paleomagnetic age reversals [*Channell et al.*, 2003] that are in good agreement with nannofossil datum levels [*Marino and Flores*, 2002]. The Site 1265 age model from 33 to 34 Ma is based primarily on nannofossil and paleomagnetic data [*Zachos et al.*, 2004, chap. 6]. The oldest 200 kyr interval for Site 1265 (34–34.2 Ma) is correlated to the benthic foraminiferal $\delta^{13}C$ record from Site 1090 to account for potential reworking.

2.2. Analytical Methods

[14] Sites 1090 and 1265 sediment samples were disaggregated in buffered water and washed through a 63 μm mesh sieve. Washed samples were dry sieved through a 150 μm sieve and five to ten benthic foraminiferal specimens of the epifaunal genus *Cibicidoides* were picked from each sample for stable isotope analysis. Approximately 100 μg of sample was dissolved in 100% phosphoric acid and analyzed for oxygen and carbon stable isotopes using a GV-Isoprime stable isotope mass spectrometer. Isotope values are reported
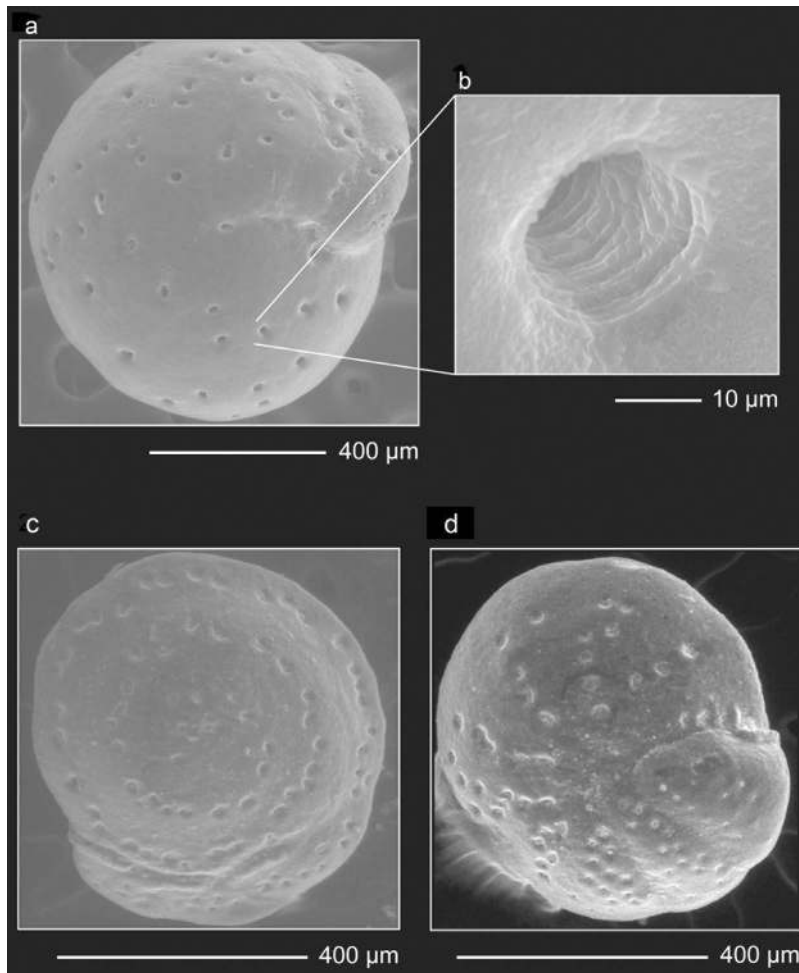

Figure 2. SEM images of Ocean Drilling Program Sites 1090 and 1265 benthic foraminiferal specimens from the genus *Cibicidoides* at 228.24 and 186.58 m composite depth (mcd), respectively. (a) ODP Site 1090 *Cibicidoides grimsdalei* SEM image at 400 μms from 228.24 mcd with 30 weight percent $CaCO_3$ [*Latimer and Filippelli*, 2002]. (b) ODP Site 1090 *Cibicidoides grimsdalei* SEM image at 10 μms from 228.24 mcd with 30 weight percent $CaCO_3$ [*Latimer and Filippelli*, 2002]. (c) ODP Site 1265 *Cibicidoides praemundulus* SEM image at 400 μms showing spiral side of foraminifera from 186.58 mcd with 85 weight percent $CaCO_3$ [*Kroon et al.*, 2006]. (d) ODP Site 1265 *Cibicidoides praemundulus* SEM image at 400 μms showing umbilical side of foraminifera from 186.58 mcd with 85 weight percent $CaCO_3$ [*Kroon et al.*, 2006].

relative to the VPDB (Vienna PeeDee belemnite) standard ($\delta^{18}O = -2.20‰$ and $\delta^{13}C = 1.95‰$; following *Coplen et al.* [1983]). Replicate analysis of our standard yields an analytical precision (1σ) of 0.06‰ for oxygen and 0.05‰ for carbon. A portion of the Site 1090 samples (35 to 33.4 Ma) were analyzed on a Micromass Optima mass spectrometer at Rutgers University using procedures similar to those described above. The laboratory standard was checked regularly against NBS-19, which has a $\delta^{18}O$ offset equal to 0.04‰ and a $\delta^{13}C$ offset of 0.10‰. The laboratory standard error (1σ) is equal to 0.08‰ for $\delta^{18}O$ and 0.05‰ for $\delta^{13}C$.

[15] Five to ten individual benthic foraminifera were cleaned for trace metal analysis with both the reductive and oxidative steps outlined by *Boyle and Keigwin* [1985]. Foraminiferal tests (300–400 μg) were crushed prior to cleaning to ensure homogenization. Each cleaned sample was dissolved in 500–800 μL of 5% HNO_3 to yield a calcium concentration of approximately 80 ppm. Magnesium and calcium were measured simultaneously on a Jobin Yvon Ultima Inductively Coupled Plasma Atomic Emission Spectrophotometer (ICP-AES). Replicate analyses of a standard solution produced an analytical precision of 0.4%. Duplicate trace metal analyses performed downcore on 10% of the benthic foraminiferal samples resulted in an average reproducibility of ±0.11 mmol/mol for Site 1265 and ±0.17 mmol/mol for Site 1090 (Figure S3 in the auxiliary material).

2.3. Mg-Temperature Calibration

[16] We utilized the Mg/Ca temperature calibration developed by *Raitzsch et al.* [2008] for the benthic foraminiferal species *Cibicidoides mundulus*,

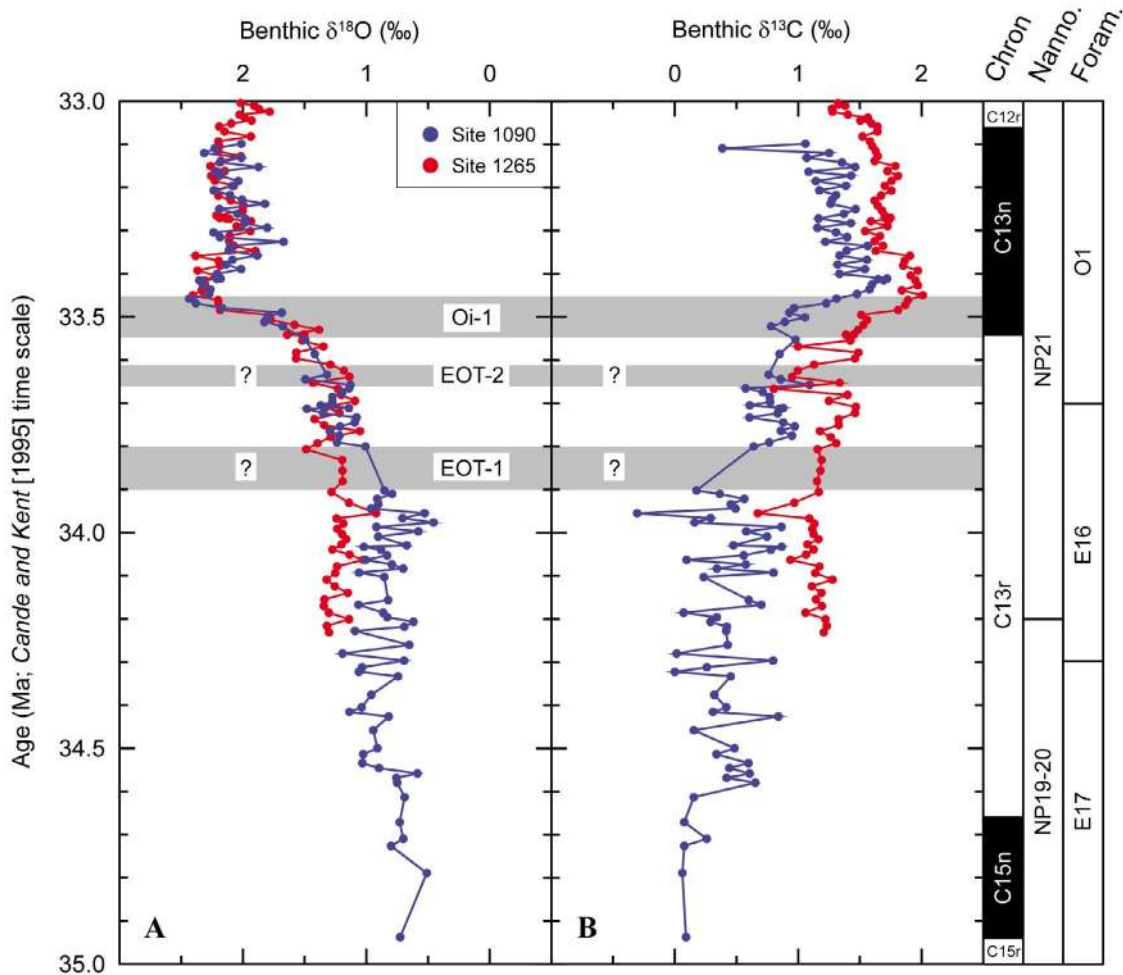$$Mg/Ca = 0.627 \exp(0.143 \times BWT), \tag{1}$$

Figure 3. ODP Sites 1090 and 1265 benthic foraminiferal stable isotope records across the Eocene-Oligocene transition. (a) Sites 1090 (blue circles) and 1265 (red circles) benthic foraminiferal (*Cibicidoides* spp.) $\delta^{18}O$ data verses age in millions of years. (b) Sites 1090 and 1265 benthic (*Cibicidoides* spp.) foraminiferal $\delta^{13}C$ data. Oxygen and carbon isotope values are reported relative to the VPDB (Vienna PeeDee belemnite) standard. Gray bars mark the EOT-1 (Eocene-Oligocene transition event 1), EOT-2 (Eocene-Oligocene transition event 2), and Oi-1 (Oligocene isotope event 1) events occurring at 33.8, 33.63, and 33.54 Ma, respectively [*Miller et al.*, 1991, 2008; *Lear et al.*, 2004; *Coxall et al.*, 2005; *Katz et al.*, 2008]. The biomagnetostratigraphic age model follows *Berggren et al.* [1995], *Cande and Kent* [1995], and *Berggren and Pearson* [2005].

where Mg/Ca and BWT are the *C. praemundulus* Mg/Ca ratio and bottom water temperature (°C), respectively. Temperatures calculated with this equation have an uncertainty of ±1.27°C. While *Yu and Elderfield* [2008] found no correlation between the Mg/Ca ratios of *C. mundulus* and BWT, a few other studies have shown a significant correlation [*Elderfield et al.*, 2006; *Healey et al.*, 2008]. In addition, *C. mundulus* has been used successfully to reconstruct BWT changes across Neogene global climate transitions [*Lear et al.*, 2003; *Shevenell et al.*, 2008].

[17] The calibration from *Raitzsch et al.* [2008] was chosen for three reasons: (1) *C. mundulus* is considered to have evolved from *C. praemundulus* [*van Morkhoven et al.*, 1986]; (2) the equation is based on present-day bottom water temperatures between 1° and 15°C; and (3) the absolute calculated BWT are comparable to previously published latest Eocene-earliest Oligocene deep water

temperatures using stable oxygen isotopes [*Savin et al.*, 1975; *Zachos et al.*, 1994] and low-resolution benthic foraminiferal Mg/Ca records [*Lear et al.*, 2000]. Our choice of temperature calibration should have a minimal effect on the relative temperature change because the published exponential equations that are based on both mixed species of *Cibicidoides* [*Rosenthal et al.*, 1997; *Martin et al.*, 2002; *Lear et al.*, 2002; *Elderfield et al.*, 2006] and *C. mundulus* [*Lear et al.*, 2003; *Raitzsch et al.*, 2008] have similar exponential constants (0.10 to 0.11 mmol/mol). Published linear calibrations for *Cibicidoides* spp. [*Rathburn and De Deckker*, 1997] and single species, *C. mundulus* [*Healey et al.*, 2008], result in overall lower-amplitude temperature changes with the exception of the single species, *C. mundulus*, equation from *Elderfield et al.* [2006]. Furthermore, deep water temperatures during the Cenozoic are considered

to be fairly uniform throughout all of the ocean basins at any given time period [*Savin et al.*, 1975].

[18] We assumed the seawater Mg/Ca ratio was 4.3 mmol/mol at ~34 Ma [*Wilkinson and Algeo*, 1989], compared to the present-day ratio of 5.1 mmol/mol [*Broecker and Peng*, 1982; *Stanley and Hardie*, 1998]. Although there is uncertainty in calculating Cenozoic paleotemperatures due to changes in seawater Mg/Ca over time [*Lear et al.*, 2000; *Billups and Schrag*, 2002], we feel confident the relative temperature change across such a rapid event as the EOT remains unaffected by this issue because of the long residence times of Mg and Ca in the ocean [*Broecker and Peng*, 1982].

3. Results

3.1. Carbon Isotopes

[19] Site 1090 benthic foraminiferal (*Cibicidoides* spp.) $\delta^{13}C$ values vary between 0.0 and 0.7‰ from the base of the record to ~33.9 Ma (Figure 3). A 0.5‰ increase occurs within ~100 kyr beginning at ~33.9 Ma and likely corresponds to EOT-1, although the data in this interval is sparse. A second increase in benthic foraminiferal $\delta^{13}C$ of 1.0‰ begins at 33.52 Ma and is coincident with Oi-1. At the end of Oi-1, $\delta^{13}C$ values reach a maximum of 1.7‰ at ~33.41 Ma. Subsequently, benthic foraminiferal $\delta^{13}C$ decreases slightly to values between 1.0 and 1.5‰ for the youngest portion of the Site 1090 record.

[20] The Site 1265 benthic foraminiferal (*Cibicidoides* spp.) $\delta^{13}C$ record shows little variability between 34.2 and 33.8 Ma, with values of 1.0–1.2‰ (Figure 3). Benthic foraminiferal $\delta^{13}C$ values increase by ~1.2‰ over a 30 kyr period starting at ~33.65 Ma and including Oi-1 (Figure 3). As at Site 1265, benthic foraminiferal $\delta^{13}C$ ratios decrease following Oi-1 from ~2.0‰ to 1.4‰ at 33.0 Ma.

3.2. Oxygen Isotopes

[21] Site 1090 benthic foraminiferal (*Cibicidoides* spp.) $\delta^{18}O$ values from the oldest portion of the record (34–35 Ma) vary between 0.5 and 1.0‰, with no long-term trend over this one million year time interval (Figure 3). Between ~33.9–33.6 Ma, there is an increase in $\delta^{18}O$ of ~0.5‰ (Figure 3). There are no obvious shifts associated with either EOT-1 or EOT-2, although the there are limited data across the first of these events. A rapid increase in benthic foraminiferal $\delta^{18}O$ of 1.0‰ begins at 33.55 Ma and coincides with Oi-1. Following the increase during Oi-1, Site 1090 $\delta^{18}O$ values decrease slightly to values centering near 2.2‰ for the remainder of the record (Figure 3).

[22] The Site 1265 benthic foraminiferal (*Cibicidoides* spp.) $\delta^{18}O$ record is marked by relatively stable values (1.0–1.5‰) from 34.2 to 33.9 Ma (Figure 3). No apparent benthic foraminiferal $\delta^{18}O$ change occurs during EOT-2 at Site 1265, though there appears to be a minor (<0.5‰) increase spanning EOT-1 (Figure 3). The benthic foraminiferal $\delta^{18}O$ records from Sites 1265 and 1090 are offset prior to 33.8 Ma and convergence immediately above EOT-1. A rapid increase of 0.8‰ occurs at Site 1265 between 33.55 and 33.45 Ma and correlates with Oi-1. The Oi-1 shift is followed by a slight decrease between 33.45 and 33.35 Ma (Figure 3). Values range between 1.9 and 2.2‰ throughout

the youngest part of the Site 1265 benthic foraminiferal $\delta^{18}O$ record.

3.3. Comparison to Global Stable Isotope Compilations

[23] A number of studies have compiled available $\delta^{18}O$ and $\delta^{13}C$ data in order to examine global trends during the late Eocene and early Oligocene [*Miller et al.*, 1987; *Zachos et al.*, 2001; *Cramer et al.*, 2009]. To assess the reliability of the Sites 1090 and 1265 benthic foraminiferal $\delta^{18}O$ and $\delta^{13}C$ records across the EOT, we compare them to the most recent of these compilations (Figure 4) from *Cramer et al.* [2009]. Site 1090 $\delta^{18}O$ values are lower than those of the whole ocean prior to EOT-1, suggesting it is bathed in a relatively warm or fresh water mass before 33.8 Ma (Figure 4). The Site 1090 benthic foraminiferal $\delta^{13}C$ values also are at the lower end of those in the global record prior to EOT-1 but become more similar to those in the global compilation after this event. Our $\delta^{18}O$ data from Site 1265 displays good agreement with the global compilation across the entire EOT (Figure 4). Conversely, the Site 1265 $\delta^{13}C$ values are consistently at the higher end of the range of values seen in the global record (Figure 4). Based on this comparison, we are confident that the stable isotope records for Sites 1090 and 1265 are reliable indicators of past changes in water mass properties at these two locations.

3.4. Benthic Foraminiferal Mg/Ca Ratios

[24] Site 1090 benthic foraminiferal Mg/Ca ratios average 0.8 ± 0.4 mmol/mol (2 s.d.) throughout the entire record, ranging from a maximum value of 1.2 mmol/mol and minimum of 0.5 mmol/mol (Figure 5). The lowest benthic foraminiferal Mg/Ca values of 0.5 mmol/mol occur at ~33.8 Ma and subsequently increase by ~0.5 mmol/mol during Oi-1 (Figure 5). Following a 100 kyr period of relatively stable values (~0.8 mmol/mol) there is a second increase of ~0.3 mmol/mol beginning at 33.27 Ma (Figure 5). In the youngest portion of the Site 1090 record, from 33.27 to 33.1 Ma, Mg/Ca ratios average ~1.0 mmol/mol.

[25] For Site 1265, *C. praemundulus* Mg/Ca values vary between 1.1 and 2.1 mmol/mol over the entire length of the record, with the average being 1.7 ± 0.4 mmol/mol (2 s.d.) (Figure 5). The initial 500 kyr of the Site 1265 record (34.2 to 33.8 Ma) displays relatively large fluctuations that appear to track changes in the carbonate content (Figure 5). Site 1265 benthic foraminiferal Mg/Ca ratios show a brief decrease after EOT-1 from 1.6 mmol/mol at ~33.75 Ma to 1.1 mmol/mol at 33.65 Ma. Subsequently, the record displays a long-term (600 kyr) increase from 1.1 mmol/mol at 33.63 Ma to 2.1 mmol/mol at 33.21 Ma (Figure 5). The gradual Mg/Ca increase of 1.0 mmol/mol over 600 kyr encompasses the Oi-1 event identified in the $\delta^{18}O$ records (Figure 5). The remaining portion of the Site 1265 benthic foraminiferal Mg/Ca record shows minimal variability with an average of 1.7 mmol/mol from 33.2 to 33 Ma.

4. Discussion

4.1. Secular Effects of Carbonate Ion and Carbon Cycle Variations

[26] Before assessing our benthic foraminiferal $\delta^{13}C$ and Mg/Ca records from the perspective of past water mass variations, we evaluate the integrity of the data including
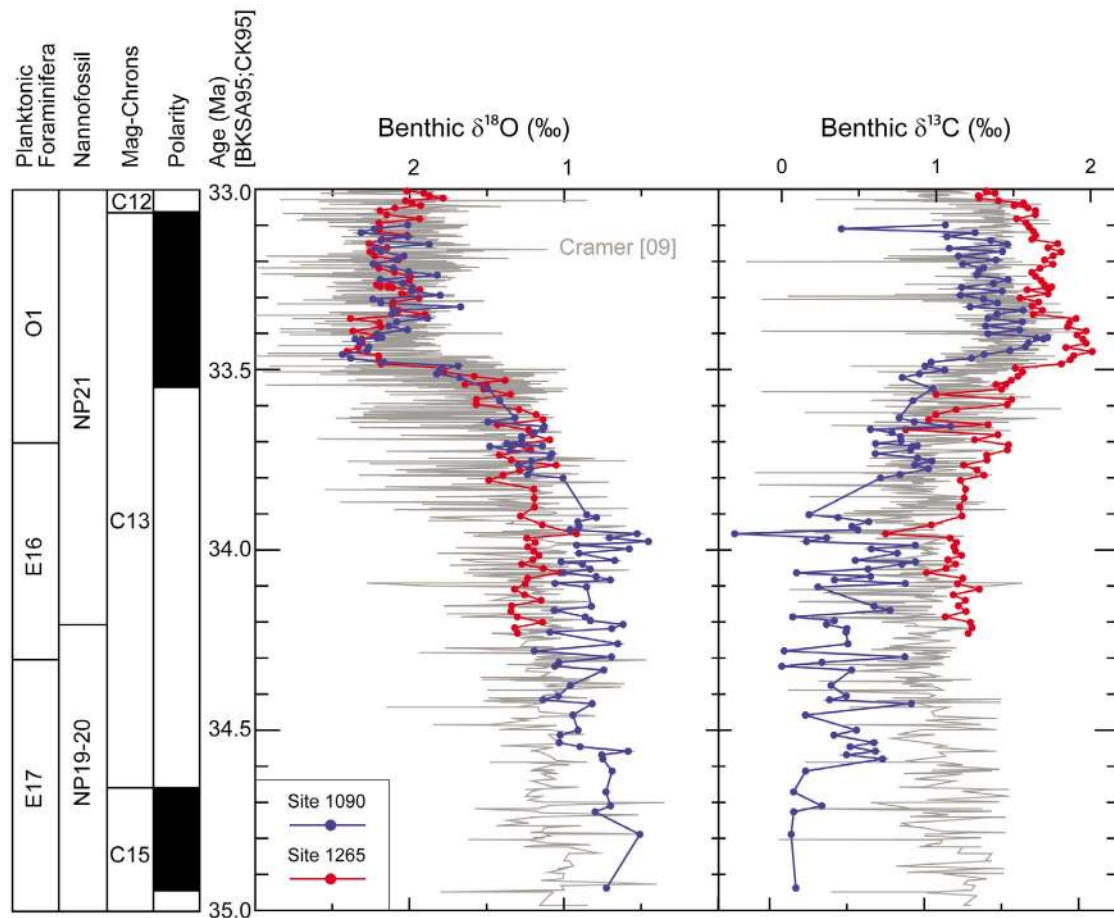
Figure 4. Benthic foraminiferal $\delta^{18}O$ and $\delta^{13}C$ isotope records across the Eocene-Oligocene transition from ODP Sites 1090 (blue circles; this work) and 1265 (red circles; this work) verses age in millions of years. The gray curve represents a recent compilation from *Cramer et al.* [2009]. Isotope values are reported relative to the VPDB (Vienna PeeDee belemnite) standard. The biomagnetostratigraphic age model follows *Berggren et al.* [1995], BKSA95; *Cande and Kent* [1995], CK95; and *Berggren and Pearson* [2005].

their use as ventilation and paleotemperature indicators. Variations in deep water $\delta^{13}C$ values reflect changes in (1) the global carbon reservoir [*Broecker*, 1970, 1982; *Shackleton*, 1977], (2) deep water circulation patterns [*Bender and Keigwin*, 1979; *Belanger et al.*, 1981; *Curry and Lohmann*, 1982, 1983; *Boyle and Keigwin*, 1982; *Shackleton et al.*, 1983], and (3) regional surface water productivity [*Sarnthein et al.*, 1982]. A global deep water $\delta^{13}C$ increase coincident with Oi-1 (Figure 3) is associated with a significant deepening of the CCD and rise in the $[CO_3^{2-}]$ of bottom waters [*van Andel*, 1975; *Zachos et al.*, 1996; *Salamy and Zachos*, 1999; *Coxall et al.*, 2005; *Zachos and Kump*, 2005; *Merico et al.*, 2008]. The earliest Oligocene benthic foraminiferal $\delta^{13}C$ increase coincides with changes in marine productivity and/or in the organic carbon to inorganic carbon burial rates in the high to middle southern latitudes [*Diester-Haass and Zahn*, 1996, 2001; *Salamy and Zachos*, 1999; *Diester-Haass and Zachos*, 2003; *Anderson and Delaney*, 2005]. Sites 1090 and 1265 benthic foraminiferal $\delta^{13}C$ records show an increase (0.5–0.7‰) coeval with Oi-1 (Figure 3) that is consistent with

other deep sea records (Figure 6) [e.g., *Miller et al.*, 1988; *Miller and Thomas*, 1985; *Barrera and Huber*, 1991; *Zachos et al.*, 1992, 1996].

[27] The proposed change in paleoproductivity and export of organic carbon relative to carbonate carbon associated with Oi-1 can be attributed to more vigorous ocean mixing rates. Considerable debate exists concerning whether a stronger meridional temperature gradient, intensified wind stress and upwelling, or the opening of tectonic gateways in the Southern Ocean caused ocean mixing rates to increase at this time [*Diester-Haass*, 1996; *Salamy and Zachos*, 1999; *Diester-Haass and Zahn*, 2001; *Diester-Haass and Zachos*, 2003; *Hay et al.*, 2005; *Latimer and Filippelli*, 2002; *Cramer et al.*, 2009].

4.2. Bottom Water Temperature and Water Mass Properties

[28] Site 1090 BWT that are uncorrected for changes in the $[CO_3^{2-}]$ range between 1° and 3°C in the early portion of the record from 34.5 to 34 Ma (Figure 7). BWT eventually increases to as warm as 5°–6°C at the top of the Site 1090
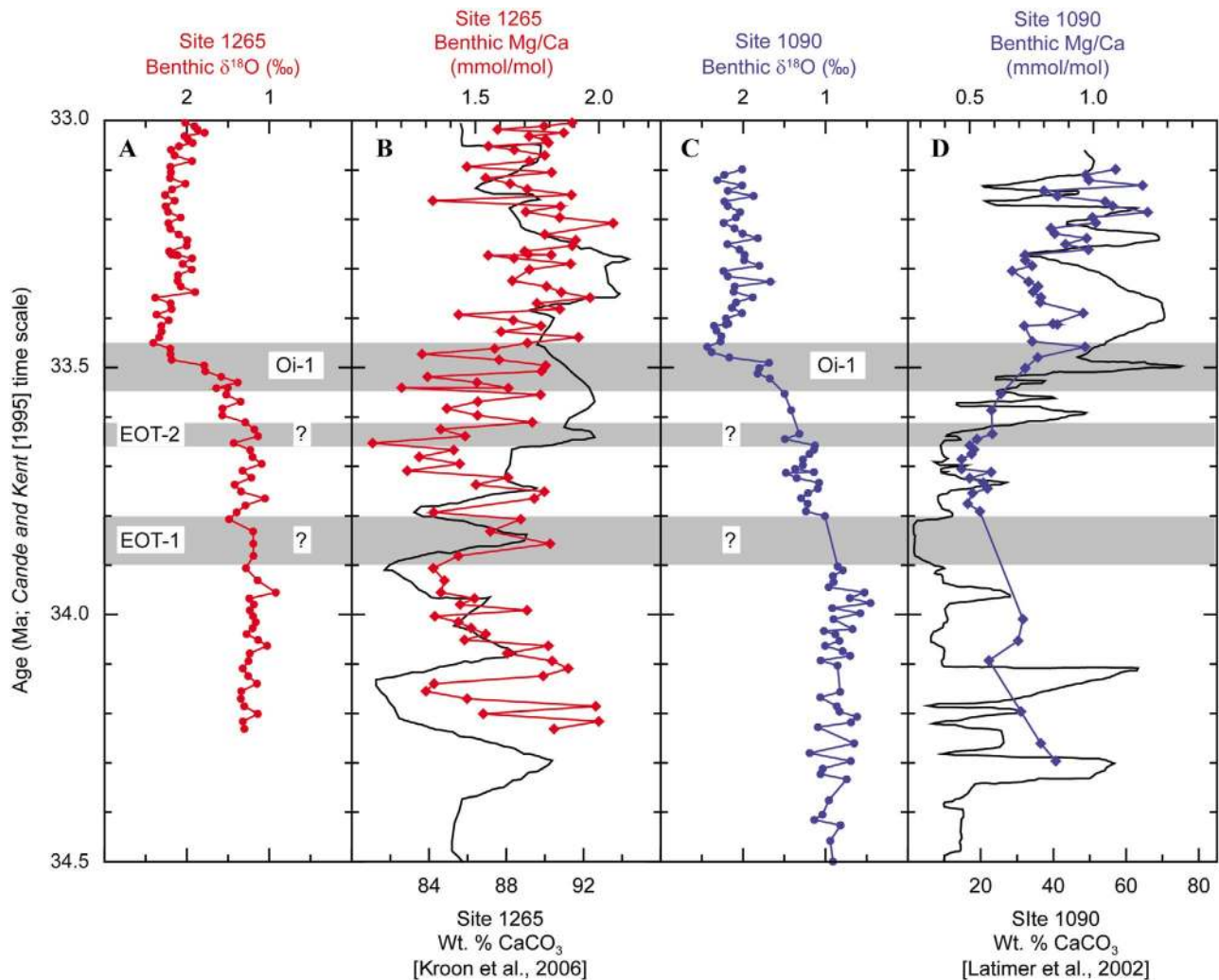
Figure 5. ODP Sites 1265 and 1090 benthic foraminiferal $\delta^{18}O$, Mg/Ca, and weight percent carbonate records verses age in millions of years. (a) Site 1265 benthic foraminiferal $\delta^{18}O$ values (red circles; *Cibicidoides* spp.) verses age in millions of years. Isotope values are reported relative to the VPDB (Vienna PeeDee belemnite) standard. (b) Site 1265 benthic foraminiferal Mg/Ca ratios (red diamonds; *C. praemundulus*) in mmol/mol plotted with weight percent carbonate (black line) from *Kroon et al.* [2006]. (c) Site 1090 benthic foraminiferal $\delta^{18}O$ values (blue circles; *Cibicidoides* spp.). (d) Site 1090 benthic foraminiferal Mg/Ca ratios (blue diamonds; *Cibicidoides* spp.) in mmol/mol plotted with weight percent carbonate (black line) from *Latimer and Filippelli* [2002]. Gray bars mark the EOT-1 (Eocene-Oligocene transition event 1), EOT-2 (Eocene-Oligocene transition event 2), and Oi-1 (Oligocene isotope event 1) events occurring at 33.8, 33.63, and 33.54 Ma, respectively [*Miller et al.*, 1991, 2008; *Lear et al.*, 2004; *Coxall et al.*, 2005; *Katz et al.*, 2008].

record (Figure 7). In contrast, Site 1265 uncorrected BWT are uniformly warmer (6°–8°C) and marked by little change throughout (Figure 7). Currently, Site 1090 BWT (1.2°C) are only slightly colder than those at Site 1265 (2.4°C) [*Levitus and Boyer*, 1994]. A ~5°C difference in uncorrected BWT between Sites 1090 and 1265 in the late Eocene and a ~1–2°C contrast in the early Oligocene suggests the two sites were bathed in different water masses prior to and following the EOT. Colder BWT at Site 1090 compared to Site 1265 associated with the EOT are supported by recent work that found a substantial $\Delta\delta^{18}O$ gradient between South and North Atlantic deep waters coincident with Oi-1 [*Cramer et al.*, 2009]. Site 1090 shows a ~2°C BWT

cooling from 34 to 33.8 Ma, the time period containing EOT-1. A 200 kyr gap in the Site 1090 BWT record, possibly due to dissolution (Figure 5), makes it impossible to constrain the timing and magnitude of change across EOT-1. At 33.8 Ma, Site 1265 BWT display a ~1°C cooling associated with EOT-1 (Figure 7).

[29] Site 1265 uncorrected BWT record shows no significant change across Oi-1 (Figure 7). In contrast, Site 1090 uncorrected BWTs display a ~3°C warming beginning at EOT-2 and extending through Oi-1 (Figure 7), which is comparable to the 2°C increase estimated for deep waters at Sites 1218 and 522 [*Lear et al.*, 2000, 2004]. A BWT warming associated with Oi-1 is likely an artifact of changes
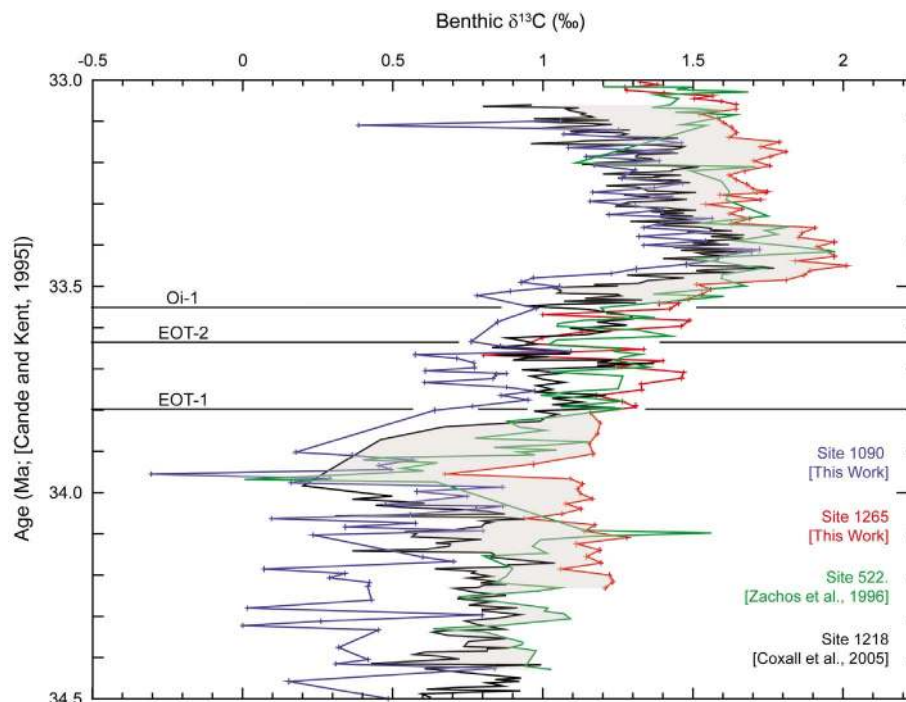
Figure 6. Summary of the latest Eocene to earliest Oligocene $\delta^{13}C$ ratios for *Cibicidoides* from Southern Ocean ODP Site 1090, east Atlantic ODP Site 1265, east Atlantic DSDP Site 522 [*Zachos et al.*, 1996], and Pacific Ocean ODP Site 1218 [*Coxall et al.*, 2005]. Site 1090 represents the Southern Ocean end-member, with Site 1218 [*Coxall et al.*, 2005] serving as the Pacific end-member for deep water during the EOT. Gray shading illustrates the influence of a more nutrient-depleted water mass at Sites 1265 and 522 [*Zachos et al.*, 1996]. The $\delta^{18}O$ and $\delta^{13}C$ values are reported relative to the VPDB (Vienna PeeDee belemnite) standard. Black horizontal lines mark the EOT-1 (Eocene-Oligocene transition event 1), EOT-2 (Eocene-Oligocene transition event 2), and Oi-1 (Oligocene isotope event 1) events occurring at 33.8, 33.63, and 33.54 Ma, respectively [*Miller et al.*, 1991, 2008; *Lear et al.*, 2004; *Coxall et al.*, 2005; *Katz et al.*, 2008].

in the $[\Delta CO_3^{2-}]$ of the oceans coincident with the EOT [*Lear et al.*, 2004; *Lear and Rosenthal*, 2006; *Peck et al.*, 2010; *Lear et al.*, 2010]. An abrupt (<300 kyr) deepening (1.2 km) of the CCD occurred throughout the global ocean near the E-O boundary [*van Andel*, 1975; *Rea and Lyle*, 2005; *Coxall et al.*, 2005]. A rise in bottom water $[CO_3^{2-}]$ has been shown to cause an increase in benthic foraminiferal Mg/Ca ratios [*Elderfield et al.*, 2006; *Rosenthal et al.*, 2006; *Healey et al.*, 2008; *Yu and Elderfield*, 2008], which in turn yield temperature estimates that are anomalously high.

[30] A change in $[\Delta CO_3^{2-}]$ may have affected the deeper of the two sites (Site 1090) more dramatically as evidenced by higher CaCO$_3$ percentages at Site 1265 (85–95%) relative to those at Site 1090 (5–40%) across the entire EOT interval (Figure 5). Nearby ODP Site 1263 (28°31.9′S, 2°46.7′E) was determined to be above the lysocline at 2.1 km paleodepth at ~34 Ma [*Peck et al.*, 2010]. *Peck et al.* [2010] estimated a ~29 μmol/kg $[CO_3^{2-}]$ increase in bottom waters at Site 1263 associated with Oi-1. A ~29 μmol/kg $[CO_3^{2-}]$ change is equivalent to a Mg/Ca ratio increase of ~0.25 mmol/mol using the relationship of 0.0086 mmol/mol per μmol/kg from *Elderfield et al.* [2006]. Correcting our Site 1265 Mg/Ca deep water record for a ~0.25 mmol/mol increase yields BWT estimates that show a ~1.5°C cooling beginning at ~33.6 Ma and culminating at Oi-1 (Figure 8).

Site 1090 Mg/Ca ratios are corrected for a larger change in the $[CO_3^{2-}]$ because it is the deeper of the two sites located at 3.2 km paleodepth at ~34 Ma and the CaCO$_3$ weight percent varies significantly more than Site 1265 (Figure 5). Site 1090 is adjusted for a 0.31 mmol/mol Mg/Ca increase [*Elderfield et al.*, 2006] (Figure 8) based on a ~36 μmol/kg $[CO_3^{2-}]$ change identified at equatorial Pacific ODP Site 1218 (4 km paleodepth at 34 Ma) across Oi-1 [*Lear et al.*, 2010]. Corrected Mg/Ca values for Site 1090 (Figure 8) yield a ~1.5°C BWT decrease associated with Oi-1, similar to that for Site 1265.

[31] Our reconstructed Mg/Ca BWT records for Sites 1090 and 1265 can be used in conjunction with the benthic foraminiferal $\delta^{13}C$ data to postulate the source regions for deep water masses at these two locations during the EOT [*Bender and Keigwin*, 1979; *Curry and Lohmann*, 1982, 1983; *Boyle and Keigwin*, 1982; *Shackleton et al.*, 1983; *Mix and Fairbanks*, 1985; *Oppo and Fairbanks*, 1987]. At present, Site 1265 is bathed by nutrient-depleted North Atlantic Deep Water (NADW) with a $\delta^{13}C$ value of ~1.0‰ [*Kroopnick*, 1985]. Likewise, Site 1090 is currently located in the mixing zone between NADW and lower Circumpolar Deep Water, with a $\delta^{13}C$ value of ~0.4‰ [*Kroopnick*, 1985]. The principle region for deep water formation during the early Paleogene was the Southern Ocean [*Miller and*
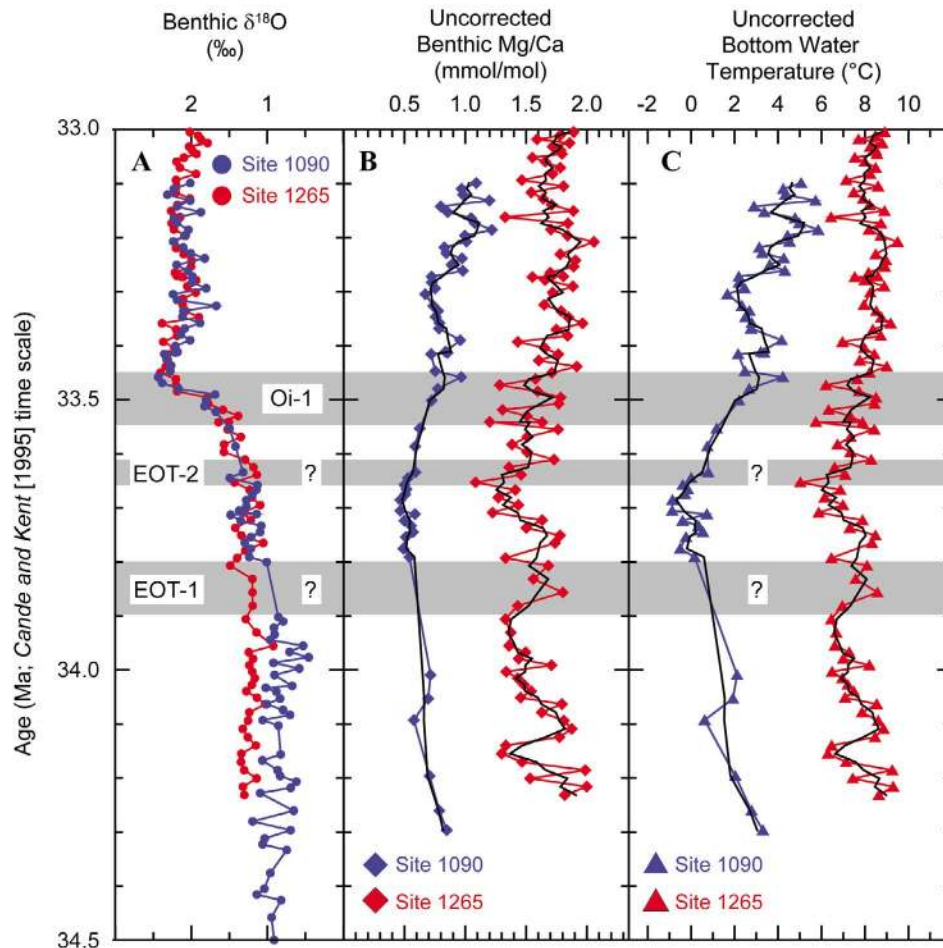
Figure 7. ODP Sites 1090 and 1265 benthic foraminiferal δ^{18}O, uncorrected Mg/Ca, and uncorrected bottom water temperature (BWT) records verses age in millions of years. (a) Benthic foraminiferal (*Cibicidoides* spp.) δ^{18}O records from Sites 1090 (blue circles) and 1265 (red circles). Isotope values are reported relative to the VPDB (Vienna PeeDee belemnite) standard. (b) Sites 1090 (blue diamonds; *Cibicidoides* spp.) and 1265 (red diamonds; *C. praemundulus*) benthic foraminiferal Mg/Ca ratios in mmol/mol uncorrected for changes in the deep water carbonate ion concentration associated with Oi-1 [*Peck et al.*, 2010; *Lear et al.*, 2010]; black lines show three-point running average. (c) Unadjusted bottom water temperatures (Site 1090, blue triangles; Site 1265, red triangles) calculated from uncorrected benthic foraminiferal Mg/Ca data in Figure 7b using the benthic foraminiferal calibration of *Raitzsch et al.* [2008] with the modern-day Mg/Ca seawater value (5.1 mmol/mol) and assuming Mg/Ca = 4.3 mmol/mol at 34 Ma; black lines display three-point running average. Gray bars mark the EOT-1 (Eocene-Oligocene transition event 1), EOT-2 (Eocene-Oligocene transition event 2) and Oi-1 (Oligocene isotope event 1), events occurring at 33.8, 33.63, and 33.54 Ma, respectively [*Miller et al.*, 1991, 2008; *Lear et al.*, 2004; *Coxall et al.*, 2005; *Katz et al.*, 2008].

Tucholke, 1983; *Mountain and Miller*, 1992; *Pak and Miller*, 1992; *Thomas et al.*, 2003; *Via and Thomas*, 2006]. Some studies from the North Atlantic suggest a Northern Component Water mass (NCW; ancient analog to NADW [*Wright et al.*, 1991]), probably originating in the Norwegian Sea, was produced in the early Oligocene and the latest Eocene [*Miller and Tucholke*, 1983; *Miller*, 1992; *Wold*, 1994].

[32] Sites 1090 and 1265 benthic foraminiferal δ^{13}C records are compared with two high-resolution EOT δ^{13}C records (Figure 6) from equatorial Pacific Site 1218 (4 km paleodepth) [*Coxall et al.*, 2005] and South Atlantic Site 522 (3 km paleodepth) [*Zachos et al.*, 1996] (Figure 1).

Throughout the entire study interval, Site 1265 benthic δ^{13}C values are higher than those at both Site 1090 and Site 1218, but often similar to those for Site 522 (Figure 6). Site 1090 is marked by relatively low (0.4‰) benthic δ^{13}C values prior to EOT-1 that are comparable to the modern-day Circumpolar Deep Waters [*Kroopnick*, 1985]. In contrast, Site 1265 benthic δ^{13}C values are consistently 1.0‰ or higher, which would be indicative of a more nutrient-depleted water mass, most likely from a northern source region. In Figure 6, Site 1090 is considered to represent the Southern Ocean end-member, with Site 1218 [*Coxall et al.*, 2005] serving as the Pacific end-member for deep water during the latest Eocene-earliest Oligocene. Sites 522
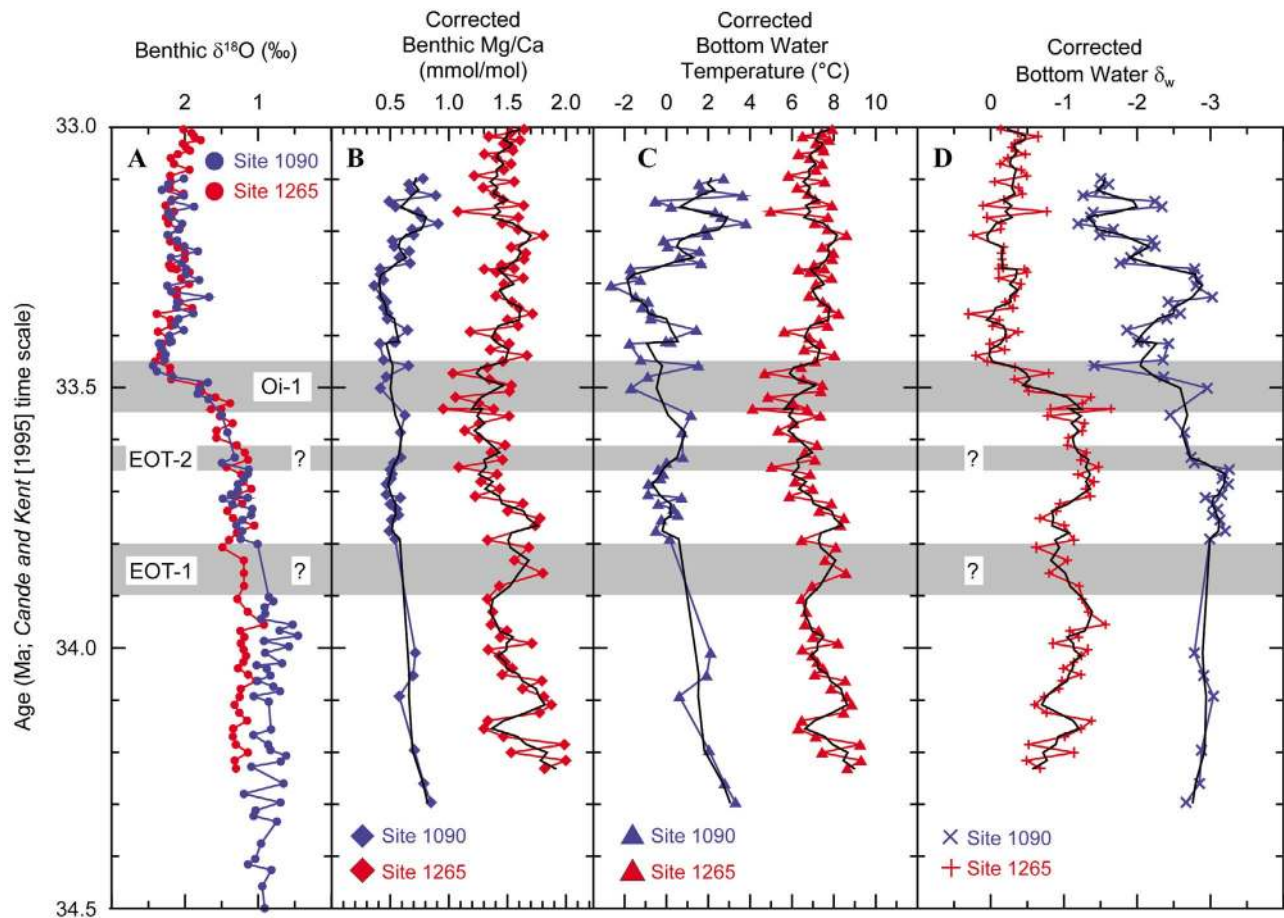
Figure 8. ODP Sites 1090 and 1265 benthic foraminiferal δ^{18}O, corrected Mg/Ca, corrected bottom water temperature (BWT), and corrected seawater δ^{18}O records verses age in millions of years. (a) Benthic foraminiferal (*Cibicidoides* spp.) δ^{18}O records from Sites 1090 (blue circles) and 1265 (red circles). Isotope values are reported relative to the VPDB (Vienna PeeDee belemnite) standard. (b) Sites 1090 (blue diamonds; *Cibicidoides* spp.) and 1265 (red diamonds; *C. praemundulus*) benthic foraminiferal Mg/Ca ratios in mmol/mol corrected for changes in the deep water carbonate ion concentration associated with Oi-1 [*Peck et al.*, 2010; *Lear et al.*, 2010]; black lines show three-point running average. (c) Adjusted bottom water temperatures (BWT) corrected for changes in the carbonate ion concentration from Sites 1090 (blue triangles) and Site 1265 (red triangles) calculated from adjusted benthic foraminiferal Mg/Ca data in Figure 8b using the benthic foraminiferal calibration of *Raitzsch et al.* [2008] with the modern-day Mg/Ca seawater value (5.1 mmol/mol) and assuming Mg/Ca = 4.3 mmol/mol at 34 Ma; black lines display three-point running average. (d) Corrected bottom water δ^{18}O (δ_w) calculated from benthic foraminiferal δ^{18}O data in Figure 8a and adjusted BWT in Figure 8c using the equation of *Shackleton* [1974]. Gray bars mark the EOT-1 (Eocene-Oligocene transition event 1), EOT-2 (Eocene-Oligocene transition event 2), and Oi-1 (Oligocene isotope event 1) events occurring at 33.8, 33.63, and 33.54 Ma, respectively [*Miller et al.*, 1991, 2008; *Lear et al.*, 2004; *Coxall et al.*, 2005; *Katz et al.*, 2008].

[*Zachos et al.*, 1996] and 1265 have similar δ^{13}C values prior to EOT-1 and following Oi-1 (Figure 6), likely indicating the presence of northern sourced waters at these two locations prior to EOT-1 and in the earliest Oligocene (Figure 6).

[33] A late Eocene to early Oligocene age for deep water formation in the North Atlantic is considerably older than most previous estimates from benthic foraminiferal δ^{13}C and faunal studies [e.g., *Schnitker*, 1980; *Wright et al.*, 1992; *Wright and Miller*, 1996]. Our benthic δ^{13}C record for Site 1265 is consistent with the presence of nutrient-depleted

northern sourced water at 2400 m depth in the South Atlantic in the earliest Oligocene (Figure 6). Neodymium isotope records support an early Oligocene age for NCW export production [*Scher and Martin*, 2004; *Via and Thomas*, 2006]. Likewise, recent seismic stratigraphic studies from the Southeast Faeroes drift and the northwestern Rockall Trough report an age of 35 Ma in late Eocene for the presence of NCW [*Davies et al.*, 2001; *Howe et al.*, 2001], consistent with prior studies from the northern North Atlantic that noted an erosional pulse associated with reflector R4 spanning the Eocene/Oligocene boundary

[*Miller and Tucholke*, 1983]. A potential mechanism for the southward penetration of NCW is revealed in sedimentary records from DSDP Site 336 that show rapid subsidence of the Greenland-Scotland Ridge from 36 to 32 Ma that allowed deep waters to spill into the North Atlantic from the Norwegian Sea [*Abelson et al.*, 2008].

4.3. Seawater $\delta^{18}O$, Sea Level, and Global Ice Volume

[34] Utilizing the Mg/Ca BWT estimates corrected for changes in the $[CO_3^{2-}]$, we attempt to partition the benthic foraminiferal $\delta^{18}O$ records into their temperature and ice volume components. The $\delta^{18}O$ of bottom water (δ_w) for Sites 1090 and 1265 is estimated using the equation below from *Shackleton* [1974]:

$$\delta_w = \delta_c - [(16.9 - T)/4], \qquad (2)$$

where T and δ_c are the *C. praemundulus* corrected Mg/Ca temperature and $\delta^{18}O$, respectively.

[35] While the Site 1090 δ_w record lacks data across EOT-1, Site 1265 displays a small δ_w increase of ~0.5‰ (Figure 8). The estimated 2°C BWT cooling during EOT-1 in the Site 1090 corrected Mg/Ca record would be equivalent to a benthic foraminiferal $\delta^{18}O$ shift of ~0.5‰, which is virtually the entire measured change. Thus, we conclude that EOT-1 is primarily a cooling event accompanied by minimal ice growth.

[36] The Site 1265 δ_w record adjusted for changes in the $[CO_3^{2-}]$ shows a larger shift (~1.0‰) than for Site 1090 (~0.5‰) across Oi-1 (Figure 8). The average δ_w shift across Oi-1 for Sites 1090 and 1265 is ~0.75‰, which equates to an average ~70 m drop in sea level, using either the Pleistocene sea level δ_w calibration of 0.11‰/10 m [*Fairbanks and Matthews*, 1978] or the Oligocene calibrations of 0.10‰/10 m [*Pekar et al.*, 2002; *DeConto and Pollard*, 2003; *Katz et al.*, 2008]. A 0.5 to 1.0‰ δ_w shift at Sites 1090 and 1265 equates to a minimum 45 m and maximum 90 m eustatic fall coincident with Oi-1. An average global sea level fall of ~70 m is comparable to earlier independent estimates of a 55–70 m drop associated with Oi-1 determined at other locations using different techniques [*Pekar et al.*, 2002; *Miller et al.*, 2005; *Katz et al.*, 2008].

[37] We estimate an average ice volume increase of 21×10^6 km³ associated with Oi-1 based on a value of −50‰ for the Antarctic ice sheet $\delta^{18}O$ [*Shackleton and Kennett*, 1975] and a 0.75‰ change in the δ_w of the oceans. Our ice volume calculation assumes an ice-free world with an average oceanic $\delta^{18}O$ composition of −1.2‰ and total water volume of 1.39×10^9 km³ [*Shackleton and Kennett*, 1975]. Using the δ_w changes at Sites 1090 and 1265, we estimate the volume of ice on Antarctic coincident with Oi-1 ranged from of 14×10^6 km³ to 28×10^6 km³, which is equivalent to ~55 to 115% of the present-day ice sheet [*Lythe et al.*, 2001] with ~85% being the average value. Alternately, a less depleted $\delta^{18}O$ value (−45‰) has been proposed for the earliest Oligocene ice sheet based on evidence for lower $\delta^{18}O$ precipitation values during late Early Cretaceous caused by an intensified hydrologic cycle [*White et al.*, 2001]. A lower ice sheet $\delta^{18}O$ value of −45‰ yields an average ice volume of 23×10^6 km³ that is equivalent to nearly 95% of today's Antarctic ice sheet. We find an ear-

liest Oligocene Antarctic ice sheet of 55–115% of its present-day size plausible based on the recent work from *Wilson and Luyendyk* [2009] that suggests the West Antarctic landmass was 10–20% larger in area during the latest Eocene.

5. Conclusions

[38] While it has long been recognized that major climate reorganization occurred at the EOT, it has been difficult to differentiate temperature and ice volume changes associated with this event. Our results from ODP Sites 1090 and 1265 show a 0.5‰ $\delta^{18}O$ increase associated with EOT-1 (33.8 Ma) that reflects a 2°C global cooling event based on benthic foraminiferal Mg/Ca data, with little if any ice growth and sea level change at this time. Our uncorrected Mg/Ca records yield a 3°C warming of bottom water temperatures that are concurrent with Oi-1. The absence of bottom water cooling coincident with Oi-1 is consistent with other deep sea records (i.e., Sites 522 and 1218) [*Lear et al.*, 2000, 2004], but is most likely an artifact of a deepening of the CCD at this time [*van Andel*, 1975; *Rea and Lyle*, 2005; *Coxall et al.*, 2005]. Sites 1090 and 1265 BWT and benthic $\delta^{13}C$ records provide evidence for a pulse of Northern Component Water prior to and following the EOT. Reconstructed BWT and seawater δ_w records corrected for a change in the $[CO_3^{2-}]$ show a ~1.5°C cooling and simultaneous 0.75‰ δ_w average increase coincident with Oi-1. The 0.75‰ δ_w increase during Oi-1 is equivalent to a ~70 m mean eustatic lowering and an ice volume change that is 85–95% of the modern Antarctic ice sheet.

References

Abelson, M., A. Agnon, and A. Almogi-Labin (2008), Indications for control of the Iceland plume on the Eocene-Oligocene "greenhouse-icehouse" climate transition, *Earth Planet. Sci. Lett.*, *265*, 33–48, doi:10.1016/j.epsl.2007.09.021.

Anderson, L. D., and M. L. Delaney (2005), Use of multiproxy records on the Agulhas Ridge, Southern Ocean (Ocean Drilling Project Leg 177, Site 1090) to investigate sub-Antarctic hydrography from the Oligocene to the early Miocene, *Paleoceanography*, *20*, PA3011, doi:10.1029/2004PA001082.

Baker, P., J. Gieskes, and H. Elderfield (1982), Diagenesis of carbonates in deep-sea sediments-Evidence from Sr/Ca ratios and interstitial dissolved Sr^{2+} data, *J. Sediment. Petrol.*, *52*, 71–82.

Barrera, E., and B. T. Huber (1991), Paleogene and early Neogene oceanography of the Southern Ocean: Leg 119 foraminifer stable isotope results, *Proc. Ocean Drill. Program, Sci. Results*, *119*, 693–717.

Belanger, P. E., W. B. Curry, and R. K. Matthews (1981), Core-top evaluation of benthic foraminiferal isotopic ratios for paleo-oceanographic interpretations, *Palaeogeogr. Palaeoclimatol. Palaeoecol.*, *33*, 205–220, doi:10.1016/0031-0182(81)90039-0.

Bender, M. L., and L. D. Keigwin (1979), Speculations about the upper Miocene change in abyssal Pacific dissolved bicarbonate $\delta^{13}C$, *Earth Planet. Sci. Lett.*, *45*, 383–393, doi:10.1016/0012-821X(79)90138-9.

Berger, W. H. (1982), Deep-sea stratigraphy: Cenozoic climate steps and the search for chemoclimatic feedback, in *Cyclic and Event Stratification*, edited by G. Einsele and A. Sielacher, pp. 121–157, Springer, New York.

Berggren, W. A., and P. N. Pearson (2005), A revised tropical to subtropical Paleogene planktonic foraminiferal zonation, *J. Foraminiferal Res.*, 35(4), 279–298, doi:10.2113/35.4.279.

Berggren, W. A., D. V. Kent, C. C. Swisher, and M.-P. Aubry (1995), A revised Cenozoic geochronology and chronostratigraphic, in *Geochronology, Time Scales and Global Stratigraphic Correlations*, edited by W. A. Berggren et al., *Spec. Publ. SEPM Soc. Sediment. Geol.*, 54, pp. 129–212.

Billups, K., and D. P. Schrag (2002), Paleotemperatures and ice volume of the past 27 Myr revisited with paired Mg/Ca and $^{18}O/^{16}O$ measurements on benthic foraminifera, *Paleoceanography*, 17(1), 1003, doi:10.1029/2000PA000567.

Billups, K., and D. P. Schrag (2003), Application of benthic foraminiferal Mg/Ca ratios to questions of Cenozoic climate change, *Earth Planet. Sci. Lett.*, 209, 181–195, doi:10.1016/S0012-821X(03)00067-0.

Boyle, E. A., and L. D. Keigwin (1982), Deep circulation of the North Atlantic over the last 200,000 years: Geochemical evidence, *Science*, 218(4574), 784–787, doi:10.1126/science.218.4574.784.

Boyle, E. A., and L. D. Keigwin (1985), Comparison of Atlantic and Pacific paleochemical records for the last 250,000 years: Changes in deep ocean circulation and chemical inventories, *Earth Planet. Sci. Lett.*, 76, 135–150, doi:10.1016/0012-821X(85)90154-2.

Broecker, W. S. (1970), A boundary condition on the evolution of atmospheric oxygen, *J. Geophys. Res.*, 75, 3553–3557, doi:10.1029/JC075i018p03553.

Broecker, W. S. (1982), Ocean chemistry during glacial time, *Geochim. Cosmochim. Acta*, 46, 1689–1705, doi:10.1016/0016-7037(82)90110-7.

Broecker, W. S., and T.-H. Peng (1982), *Tracers in the Sea*, Lamont-Doherty Earth Obs., Palisades, N. Y.

Brown, S. J., and H. Elderfield (1996), Variations in Mg/Ca and Sr/Ca ratios of planktonic foraminifera caused by post-depositional dissolution: Evidence of shallow Mg-dependent dissolution, *Paleoceanography*, 11(5), 543–551, doi:10.1029/96PA01491.

Cande, S., and D. Kent (1995), Revised calibration of the geomagnetic polarity timescale for the Late Cretaceous and Cenozoic, *J. Geophys. Res.*, 110, 6093–6095, doi:10.1029/94JB03098.

Channell, J. T., S. Galeotti, E. Martin, K. Billups, H. D. Scher, and J. S. Stoner (2003), Eocene to Miocene magnetostratigraphy, biostratigraphy, and chemostratigraphy at ODP Site 1090(sub-Antarctic South Atlantic), *Geol. Soc. Am. Bull.*, 115(5), 607–623, doi:10.1130/0016-7606(2003)115<0607:ETMMBA>2.0.CO;2.

Coplen, T. B., C. Kendall, and J. Hopple (1983), Comparison of stable isotope reference samples, *Nature*, 302, 236–238, doi:10.1038/302236a0.

Coxall, H. K., P. A. Wilson, H. Palike, C. H. Lear, and J. Backman (2005), Rapid stepwise onset of Antarctic glaciation and deeper calcite compensation in the Pacific Ocean, *Nature*, 433, 53–57, doi:10.1038/nature03135.

Cramer, B. S., J. R. Toggweiler, J. D. Wright, M. E. Katz, and K. G. Miller (2009), Ocean overturning since the Late Cretaceous: Inferences from a new benthic foraminiferal isotope compilation, *Paleoceanography*, 24, PA4216, doi:10.1029/2008PA001683.

Curry, W. B., and G. P. Lohmann (1982), Carbon isotopic changes in benthic foraminifera from the western South Atlantic: Reconstruction of glacial abyssal circulation patterns, *Quat. Res.*, 18(2), 218–235, doi:10.1016/0033-5894(82)90071-0.

Curry, W. B., and G. P. Lohmann (1983), Reduced advection into Atlantic Ocean deep eastern basins during the last glacial maximum, *Nature*, 306, 577–580, doi:10.1038/306577a0.

Davies, R., J. Cartwright, J. Pike, and C. Line (2001), Early Oligocene initiation of North Atlantic Deep Water formation, *Nature*, 410, 917–920, doi:10.1038/35073551.

DeConto, R. M., and D. Pollard (2003), Rapid Cenozoic glaciation of Antarctica triggered by declining atmospheric CO₂, *Nature*, 421, 245–249, doi:10.1038/nature01290.

DeConto, R. M., D. Pollard, P. A. Wilson, H. Pälike, C. H. Lear, and M. Pagani (2008), Thresholds for Cenozoic bipolar glaciation, *Nature*, 455, 652–656, doi:10.1038/nature07337.

Dekens, P. S., D. W. Lea, D. K. Pak, and H. J. Spero (2002), Core top calibration of Mg/Ca in tropical foraminifera: Refining paleotemperature estimation, *Geochem. Geophys. Geosyst.*, 3(4), 1022, doi:10.1029/2001GC000200.

Delaney, M. L. (1989), Temporal changes in interstitial water chemistry and calcite recrystallization in marine sediments, *Earth Planet. Sci. Lett.*, 95, 23–37, doi:10.1016/0012-821X(89)90165-9.

Diester-Haass, L. (1996), Late Eocene-Oligocene paleoceanography in the southern Indian Ocean (ODP Site 744), *Mar. Geol.*, 130(1–2), 99–119, doi:10.1016/0025-3227(95)00128-X.

Diester-Haass, L., and J. C. Zachos (2003), The Eocene-Oligocene transition in the Equatorial Atlantic (ODP Site 925), Paleoproductivity increase and positive $\delta^{13}C$ excursion, in *From Greenhouse to Icehouse*, edited by D. R. Prothero et al., pp. 397–418, Columbia Univ. Press, New York.

Diester-Haass, L., and R. Zahn (1996), Eocene-Oligocene transition in the Southern Ocean: History of water mass circulation and biological productivity, *Geology*, 24(2), 163–166, doi:10.1130/0091-7613(1996)024<0163:EOTITS>2.3.CO;2.

Diester-Haass, L., and R. Zahn (2001), Paleoproductivity increase at the Eocene- Oligocene climatic transition: ODP/DSDP sites 763 and 592, *Palaeogeogr. Palaeoclimatol. Palaeoecol.*, 172, 153–170, doi:10.1016/S0031-0182(01)00280-2.

Dittert, N., and R. Henrich (2000), Carbonate dissolution in the South Atlantic Ocean: Evidence from ultrastructure breakdown in Globigerina bulloides, *Deep Sea Res., Part I*, 47(4), 603–620, doi:10.1016/S0967-0637(99)00069-2.

Ehrmann, W. U. (1991), Implications of sediment composition on the southern Kerguelen Plateau for paleoclimate and depositional environment, *Proc. Ocean Drill. Program, Sci. Results*, 119, 185–210, doi:10.2973/odp.proc.sr.119.121.1991.

Ehrmann, W. U., and A. Mackensen (1992), Sedimentological for the formation of an East Antarctic ice sheet in Eocene/Oligocene time, *Palaeogeogr. Palaeoclimatol. Palaeoecol.*, 93, 85–112, doi:10.1016/0031-0182(92)90185-8.

Elderfield, H., and G. Ganssen (2000), Past temperature and $\delta^{18}O$ of surface ocean waters inferred from foraminiferal Mg/Ca ratios, *Nature*, 405, 442–445, doi:10.1038/35013033.

Elderfield, H., J. Yu, P. Anand, T. Kiefer, and B. Nyland (2006), Calibrations for benthic foraminiferal Mg/Ca paleothermometry and the carbonate ion hypothesis, *Earth Planet. Sci. Lett.*, 250, 633–649, doi:10.1016/j.epsl.2006.07.041.

Eldrett, J. S., I. C. Harding, P. A. Wilson, E. Butler, and A. P. Roberts (2007), Continental ice in Greenland during the Eocene and Oligocene, *Nature*, 446, 176–179, doi:10.1038/nature05591.

Fairbanks, R. G., and R. K. Matthews (1978), The marine oxygen isotopic record in Pleistocene coral, Barbados, West Indies, *Quat. Res.*, 10, 181–196, doi:10.1016/0033-5894(78)90100-X.

Flower, B. P., and J. P. Kennett (1993), Relations between Monterey Formation deposition and middle Miocene global cooling: Naples Beach section, *Calif. Geol.*, 21, 877–880, doi:10.1130/0091-7613(1993)021<0877:RBMFDA>2.3.CO;2.

Gersonde, R., et al. (1999), *Southern Ocean Paleoceanography*, *Proc. Ocean Drill. Program, Initial Rep.*, vol. 177, Ocean Drill. Program, College Station, Tex., doi:10.2973/odp.proc.ir.177.1999.

Hall, J. M., and L. H. Chan (2004), Li/Ca in multiple species of benthic and planktonic foraminifera: Thermocline, latitudinal, and glacial–interglacial variation, *Geochim. Cosmochim. Acta*, 68, 529–545, doi:10.1016/S0016-7037(03)00451-4.

Hay, W., S. Flögel, and E. Söding (2005), Is the initiation of glaciation on Antarctica related to a change in the structure of the ocean?, *Global Planet. Change*, 45, 23–33, doi:10.1016/j.gloplacha.2004.09.005.

Healey, S. L., R. C. Thunell, and B. H. Corliss (2008), The Mg/Ca-temperature relationship of benthic foraminiferal calcite: New core-top calibrations in the <4°C temperature, *Earth Planet. Sci. Lett.*, 272, 523–530, doi:10.1016/j.epsl.2008.05.023.

Henrich, R., K. H. Baumann, S. Gerhardt, M. Groger, and A. Volbers (2003), Carbonate preservation in deep and intermediate water masses in the South Atlantic: Evaluation and Geological Record (a review), in *The South Atlantic in the Late Quaternary-Reconstruction of Material Budgets and Current Systems*, edited by G. Wefer, S. Mulitza, and V. Ratmeyer, pp. 645–670, Springer, Berlin.

Hodell, D. A., C. D. Charles, and F. J. Sierro (2001), Late Pleistocene evolution of the ocean's carbonate system, *Earth Planet. Sci. Lett.*, 192, 109–124, doi:10.1016/S0012-821X(01)00430-7.

Howe, J. A., M. S. Stoker, and K. J. Woolfe (2001), Deep-marine seabed erosion and gravel lags in the northwestern Rockall Trough, North Atlantic Ocean, *J. Geol. Soc.*, 158(3), 427–438, doi:10.1144/jgs.158.3.427.

Katz, M. E., K. G. Miller, J. D. Wright, B. S. Wade, J. V. Browning, B. S. Cramer, and Y. Rosenthal (2008), Stepwise transition from the Eocene greenhouse to the Oligocene icehouse, *Nat. Geosci.*, 1, 329–334, doi:10.1038/ngeo179.

Kennett, J. P. (1977), Cenozoic evolution of Antarctic glaciation, the Circum-Antarctic Ocean, and their impact on global paleoceanography, *J. Geophys. Res.*, 82, 3843–3860, doi:10.1029/JC082i027p03843.

Kroon, D., J. C. Zachos, and C. Richter (Eds.) (2006), *Early Cenozoic Extreme Climates: The Walvis Ridge Transect Sites 1262–1267*, *Proc. Ocean Drill. Program, Sci. Results*, vol. 208, Ocean Drill. Program, College Station, Tex., doi:10.2973/odp.proc.sr.208.2006.

Kroopnick, P. M. (1985), The distribution of ^{13}C of ΣCO_2 in the world oceans, *Deep Sea Res., Part A*, 32(1), 57–84, doi:10.1016/0198-0149(85)90017-2.

Latimer, J., and G. Filippelli (2002), Eocene to Miocene terrigenous inputs and export production: Geochemical evidence from ODP Leg 177, Site 1090, *Palaeogeogr. Palaeoclimatol. Palaeoecol.*, *182*, 151–164, doi:10.1016/S0031-0182(01)00493-X.

Lea, D., T. Mashiotta, and H. Spero (1999), Controls on magnesium and strontium uptake in planktonic foraminifera as determined by live culturing, *Geochim. Cosmochim. Acta*, *63*, 2369–2379, doi:10.1016/S0016-7037(99)00197-0.

Lear, C. H., and Y. Rosenthal (2006), Benthic foraminiferal Li/Ca: Insights into Cenozoic seawater carbonate saturation state, *Geology*, *34*(11), 985–988, doi:10.1130/G22792A.1.

Lear, C. H., H. Elderfield, and P. A. Wilson (2000), Cenozoic deep-sea temperatures and global ice volumes from Mg/Ca in benthic foraminiferal calcite, *Science*, *287*(5451), 269–272, doi:10.1126/science.287.5451.269.

Lear, C. H., Y. Rosenthal, and N. Slowey (2002), Benthic foraminiferal Mg/Ca paleothermometry: A revised core-top evaluation, *Geochim. Cosmochim. Acta*, *66*(19), 3375–3387, doi:10.1016/S0016-7037(02)00941-9.

Lear, C. H., Y. Rosenthal, and J. D. Wright (2003), The closing of a seaway: Ocean water masses and global climate change, *Earth Planet. Sci. Lett.*, *210*, 425–436, doi:10.1016/S0012-821X(03)00164-X.

Lear, C. H., Y. Rosenthal, H. K. Coxall, and P. A. Wilson (2004), Late Eocene to early Miocene ice sheet dynamics and the global carbon cycle, *Paleoceanography*, *19*, PA4015, doi:10.1029/2004PA001039.

Lear, C. H., T. R. Bailey, P. N. Pearson, H. K. Coxall, and Y. Rosenthal (2008), Cooling and ice growth across the Eocene-Oligocene transition, *Geology*, *36*(3), 251–254, doi:10.1130/G24584A.1.

Lear, C. H., E. M. Mawbey, and Y. Rosenthal (2010), Cenozoic benthic foraminiferal Mg/Ca and Li/Ca records: Towards unlocking temperatures and saturation states, *Paleoceanography*, *25*, PA4215, doi:10.1029/2009PA001880.

Levitus, S., and T. P. Boyer (1994), *World Ocean Atlas 1994*, vol. 4, *Temperature*, *NOAA Atlas NESDIS*, vol. 4, 129 pp., NOAA, Silver Spring, Md.

Liu, Z., S. Tuo, Q. Zhao, X. Cheng, and W. Huang (2004), Deep-water Earliest Oligocene Glacial Maximum (EOGM) in South Atlantic, *Chin. Sci. Bull.*, *49*(20), 2190–2197.

Lythe, M. B., D. G. Vaughan, and the BEDMAP Consortium (2001), BEDMAP: A new ice thickness and subglacial topographic model of Antarctica, *J. Geophys. Res.*, *106*, 11,335–11,351, doi:10.1029/2000JB900449.

Marino, M., and J.-A. Flores (2002), Middle Eocene to early Oligocene calcareous nannofossil stratigraphy at Leg 177 Site 1090, *Mar. Micropaleontol.*, *45*, 383–398, doi:10.1016/S0377-8398(02)00036-1.

Martin, P. A., D. W. Lea, Y. Rosenthal, N. J. Shackleton, M. Sarnthein, and T. Papenfuss (2002), Quaternary deep sea temperature histories derived from benthic foraminiferal Mg/Ca, *Earth Planet. Sci. Lett.*, *198*, 193–209, doi:10.1016/S0012-821X(02)00472-7.

Merico, A., T. Tyrrell, and P. A. Wilson (2008), Eocene/Oligocene ocean de-acidification linked to Antarctic glaciation by sea-level fall, *Nature*, *452*, doi:10.1038/nature06853.

Miller, K. G. (1992), Middle Eocene to Oligocene stable isotopes, climate, and deep- water history: The Terminal Eocene Event?, in *Eocene-Oligocene Climatic and Biotic Evolution*, edited by D. R. Prothero and W. A. Berggren, pp. 160–177, Princeton Univ. Press, Princeton, N. J.

Miller, K. G., and E. Thomas (1985), Late Eocene to Oligocene benthic foraminiferal isotopic record, Site 574, equatorial Pacific, *Initial Rep. Deep Sea Drill. Proj.*, *85*, 771–777.

Miller, K. G., and B. E. Tucholke (1983), Development of Cenozoic abyssal circulation south of the Greenland-Scotland Ridge, in *Structure and Development of the Greenland-Scotland Ridge: New Methods and Concepts*, edited by M. Bott et al., *NATO Conf. Ser. IV*, 8, 549–589.

Miller, K. G., R. G. Fairbanks, and E. Thomas (1986), Benthic foraminiferal carbon isotope records and the development of abyssal circulation in the eastern North Atlantic, *Initial Rep. Deep Sea Drill. Proj.*, *94*, 981–996.

Miller, K. G., R. G. Fairbanks, and G. S. Mountain (1987), Tertiary oxygen isotope synthesis, sea level history, and continental margin erosion, *Paleoceanography*, *2*(1), 1–19, doi:10.1029/PA002i001p00001.

Miller, K. G., M. D. Feigenson, D. V. Kent, and R. K. Olsson (1988), Oligocene stable isotope (^{87}Sr/^{86}Sr, δ^{18}O, δ^{13}C) standard section, Deep Sea Drilling Project Site 522, *Paleoceanography*, *3*, 223–233, doi:10.1029/PA003i002p00223.

Miller, K. G., J. D. Wright, and R. G. Fairbanks (1991), Unlocking the icehouse: Oligocene-Miocene oxygen isotopes, eustasy, and margin erosion, *J. Geophys. Res.*, *96*, 6829–6848, doi:10.1029/90JB02015.

Miller, K. G., M. A. Kominz, J. V. Browning, J. D. Wright, G. S. Mountain, M. E. Katz, P. J. Sugarman, B. S. Cramer, N. Christie-Blick, and S. F. Pekar (2005), The Phanerozoic record of global sea-level change, *Science*, *310*(5752), 1293–1298, doi:10.1126/science.1116412.

Miller, K. G., J. V. Browning, M.-P. Aubry, B. S. Wade, M. E. Katz, A. A. Kulpecz, and J. D. Wright (2008), Eocene-Oligocene global climate and sea-level changes: St. Stephens Quarry, Alabama, *Geol. Soc. Am. Bull.*, *120*(1–2), 34–53, doi:10.1130/B26105.1.

Milliman, J. D. (1993), Production and accumulation of calcium carbonate in the ocean: Budget of a non steady state, *Global Biogeochem. Cycles*, *7*(4), 927–957, doi:10.1029/93GB02524.

Mix, A. C., and R. G. Fairbanks (1985), North Atlantic surface-ocean control of Pleistocene deep-ocean circulation, *Earth Planet. Sci. Lett.*, *73*, 231–243, doi:10.1016/0012-821X(85)90072-X.

Mountain, G. S., and K. G. Miller (1992), Seismic and geological evidence for late Paleocene-early Eocene deep water circulation in the western North Atlantic, *Paleoceanography*, *7*(4), 423–439, doi:10.1029/92PA01268.

Nurnberg, D., J. Bijma, and C. Hemleben (1996), Assessing the reliability of magnesium in foraminiferal calcite as a proxy for water mass temperatures, *Geochim. Cosmochim. Acta*, *60*, 803–814, doi:10.1016/0016-7037(95)00446-7.

Oppo, D. W., and R. G. Fairbanks (1987), Variability in the deep and intermediate water circulation of the Atlantic Ocean during the past 25,000 years: Northern Hemisphere modulation of the Southern Ocean, *Earth Planet. Sci. Lett.*, *86*, 1–15, doi:10.1016/0012-821X(87)90183-X.

Pagani, M., J. C. Zachos, K. H. Freeman, B. Tipple, and S. Bohaty (2005), Marked decline in atmospheric carbon dioxide concentrations during the Paleogene, *Science*, *309*, 600–603, doi:10.1126/science.1110063.

Pak, D. K., and K. G. Miller (1992), Paleocene to Eocene benthic foraminiferal isotopes and assemblages: Implications for deep water circulation, *Paleoceanography*, *7*(4), 405–422, doi:10.1029/92PA01234.

Pearson, P. N., G. L. Foster, and B. S. Wade (2009), Atmospheric carbon dioxide during the Eocene-Oligocene climate transition, *Nature*, *461*, 1110–1113, doi:10.1038/nature08447.

Peck, V. L., J. Yu, S. Kender, and C. R. Riesselman (2010), Shifting ocean carbonate chemistry during the Eocene-Oligocene climate transition: Implications for deep ocean Mg/Ca paleothermometry, *Paleoceanography*, *25*, PA4219, doi:10.1029/2009PA001906.

Pekar, S. F., N. Christie-Blick, M. A. Kominz, and K. G. Miller (2002), Calibration between glacial eustasy and oxygen isotopic data for the early icehouse world of the Oligocene, *Geology*, *30*(10), 903–906, doi:10.1130/0091-7613(2002)030<0903:CBEEFB>2.0.CO;2.

Raitzsch, M., H. Kuhnert, J. Groeneveld, and T. Bickert (2008), Benthic foraminifer Mg/Ca anomalies in South Atlantic core top sediments and their implications for paleothermometry, *Geochem. Geophys. Geosyst.*, *9*, Q05010, doi:10.1029/2007GC001788.

Rathburn, A. E., and P. DeDeckker (1997), Magnesium and strontium of recent benthic foraminifera from the Coral Sea, Australia and Prydz Bay, Antarctica, *Mar. Micropaleontol.*, *32*, 231–248, doi:10.1016/S0377-8398(97)00028-5.

Raymo, M. E. (1994), The Himalayas, organic carbon burial, and climate in the Miocene, *Paleoceanography*, *9*(3), 399–404, doi:10.1029/94PA00289.

Rea, D. K., and M. Lyle (2005), Paleogene calcite compensation depth in the eastern subtropical Pacific: Answers and questions, *Paleoceanography*, *20*, PA1012, doi:10.1029/2004PA001064.

Regenberg, M., D. Nürnberg, S. Steph, J. Groeneveld, D. Garbe-Schonberg, R. Tiedemann, and W.-C. Dullo (2006), Assessing the effect of dissolution on planktonic foraminiferal Mg/Ca ratios: Evidence from Caribbean core tops, *Geochem. Geophys. Geosyst.*, *7*, Q07P15, doi:10.1029/2005GC001019.

Robert, C., L. Diester-Haass, and H. Chamley (2002), Late Eocene-Oligocene oceanographic development at southern high latitudes, from terrigenous and biogenic particles: A comparison of Kerguelen Plateau and Maud Rise, ODP Sites 744 and 689, *Mar. Geol.*, *191*, 37–54, doi:10.1016/S0025-3227(02)00508-X.

Rosenthal, Y., and G. P. Lohmann (2002), Accurate estimation of sea surface temperatures using dissolution-corrected calibrations for Mg/Ca paleothermometry, *Paleoceanography*, *17*(3), 1044, doi:10.1029/2001PA000749.

Rosenthal, Y., E. A. Boyle, and N. Slowey (1997), Environmental controls on the incorporation of Mg, Sr, F and Cd into benthic foraminiferal shells from Little Bahama Bank: Prospects for thermocline paleoceanography, *Geochim. Cosmochim. Acta*, *61*, 3633–3643, doi:10.1016/S0016-7037(97)00181-6.

Rosenthal, Y., G. P. Lohmann, K. C. Lohmann, and R. M. Sherrell (2000), Incorporation and preservation of Mg in *Globigerinoides sacculifer*: Implications for reconstructing the temperature and ^{18}O/^{16}O of seawater, *Paleoceanography*, *15*(1), 135–145, doi:10.1029/1999PA000415.

Rosenthal, Y., C. H. Lear, D. W. Oppo, and B. Linsley (2006), Temperature and carbonate ion effects on Mg/Ca and Sr/Ca ratios in benthic fora-

minifera: Aragonitic species *Hoeglundina elegans*, *Paleoceanography*, *21*, PA1007, doi:10.1029/2005PA001158.

Salamy, K. A., and J. C. Zachos (1999), Latest Eocene-Early Oligocene climate change and Southern Ocean fertility: Inferences from sediment accumulation and stable isotope data, *Palaeogeogr. Palaeoclimatol. Palaeoecol.*, *145*, 61–77, doi:10.1016/S0031-0182(98)00093-5.

Sarnthein, M., J. Thiede, U. Pflaumann, H. Erlenkeuser, D. Futterer, B. Koopmann, H. Lange, and E. Seibold (1982), Atmospheric and oceanic circulation patterns off northwest Africa during the past 25 million years, in *Geology of the Northwest African Continental Margin*, edited by U. von Rad et al., pp. 545–604, Springer, New York.

Savin, S. M., R. G. Douglas, and F. G. Stehli (1975), Tertiary marine paleotemperatures, *Geol. Soc. Am. Bull.*, *86*(11), 1499–1510, doi:10.1130/0016-7606(1975)86<1499:TMP>2.0.CO;2.

Scher, H. D., and E. E. Martin (2004), Circulation in the Southern Ocean during the Paleogene inferred from neodymium isotopes, *Earth Planet. Sci. Lett.*, *228*, 391–405, doi:10.1016/j.epsl.2004.10.016.

Schnitker, D. (1980), North Atlantic oceanography as possible cause of Antarctic glaciation and eutrophication, *Nature*, *284*, 615–616, doi:10.1038/284615a0.

Shackleton, N. J. (1974), Attainment of isotopic equilibrium between ocean water and the benthonic foraminifera genus *Uvigerina*: Isotopic changes in the ocean during the last glacial, *Colloq. Int. CNRS*, *219*, 203–209.

Shackleton, N. J. (1977), Carbon-13 in Uvigerina: Tropical rain forest history and the equatorial Pacific carbonate dissolution cycles, in *The Fate of Fossil Fuel CO_2 in the Oceans*, edited by N. R. Anderson and A. Malahoff, pp. 401–427, Plenum, New York.

Shackleton, N. J., and J. P. Kennett (1975), Paleotemperature history of the Cenozoic and initiation of Antarctic glaciations: Oxygen and carbon isotopic analyses in DSDP Sites 277, 279, and 281, *Initial Rep. Deep Sea Drill. Proj.*, *29*, 743–755, doi:10.2973/dsdp.proc.29.117.1975.

Shackleton, N. J., J. Imbrie, and M. A. Hall (1983), Oxygen and carbon isotope record of East Pacific core V19-30: Implications for the formation of deep water in the late Pleistocene, *Earth Planet. Sci. Lett.*, *65*, 233–244, doi:10.1016/0012-821X(83)90162-0.

Shevenell, A. E., J. P. Kennett, and D. W. Lea (2008), Middle Miocene ice sheet dynamics, deep-sea temperatures, and carbon cycling: A Southern Ocean perspective, *Geochem. Geophys. Geosyst.*, *9*, Q02006, doi:10.1029/2007GC001736.

Stanley, S. M., and L. A. Hardie (1998), Secular oscillations in the carbonate mineralogy or reef-building and sediment producing organisms driven by tectonically forced shifts in seawater chemistry, *Palaeogeogr. Palaeoclimatol. Palaeoecol.*, *144*, 3–19, doi:10.1016/S0031-0182(98)00109-6.

Stein, C. A., and S. Stein (1992), A model for the global variation in oceanic depth and heat flow with lithospheric age, *Nature*, *359*, 123–129, doi:10.1038/359123a0.

Thomas, D. J., T. J. Bralower, and C. E. Jones (2003), Neodymium isotopic reconstruction of late Paleocene-early Eocene thermohaline circulation, *Earth Planet. Sci. Lett.*, *209*, 309–322, doi:10.1016/S0012-821X(03)00096-7.

Tripati, A., J. Backman, H. Elderfield, and P. Ferretti (2005), Eocene bipolar glaciations associated with global carbon cycle changes, *Nature*, *436*, 341–346, doi:10.1038/nature03874.

van Andel, T. H. (1975), Mesozoic/Cenozoic calcite compensation depth and the global distribution of calcareous sediments, *Earth Planet. Sci. Lett.*, *26*, 187–194, doi:10.1016/0012-821X(75)90086-2.

van Morkhoven, F. P. C. M., W. A. Berggren, and A. S. Edwards (1986), Cenozoic Cosmopolitan Deep-Water Benthic Foraminifera, *Bull. Cent. Rech. Explor. Prod. Elf Aquitaine*, vol. *11*, 421 pp.

Via, R. K., and D. J. Thomas (2006), Evolution of Atlantic thermohaline circulation: Early Oligocene onset of deep-water production in the North Atlantic, *Geology*, *34*(6), 441–444, doi:10.1130/G22545.1.

Vincent, E., and W. H. Berger (1985), Carbon dioxide and polar cooling in the Miocene: The Monterey hypothesis, in *The Carbon Cycle and Atmospheric CO_2: Natural Variations, Archean to Present, Geophys. Monogr. Ser*, vol. 32, edited by E. T. Sundquist and W. S. Broecker, pp. 455–468, AGU, Washington, D. C.

Volbers, A. N., and R. Henrich (2002), Present water mass calcium carbonate corrosiveness in the eastern South Atlantic inferred from ultrastructural breakdown of *Globigerina bulloides* in surface sediments, *Mar. Geol.*, *186*, 471–486, doi:10.1016/S0025-3227(02)00333-X.

White, T., L. Gonzalez, G. Ludvigson, and C. Poulsen (2001), Middle Cretaceous greenhouse hydrologic cycle of North America, *Geology*, *29*(4), 363–366, doi:10.1130/0091-7613(2001)029<0363:MCGHCO>2.0.CO;2.

Wilkinson, B. H., and T. J. Algeo (1989), Sedimentary carbonate record of calcium- magnesium cycling, *Am. J. Sci.*, *289*, 1158–1194, doi:10.2475/ajs.289.10.1158.

Wilson, D. S., and B. P. Luyendyk (2009), West Antarctic paleotopography estimated at the Eocene-Oligocene climate transition, *Geophys. Res. Lett.*, *36*, L16302, doi:10.1029/2009GL039297.

Wold, C. N. (1994), Cenozoic sediment accumulation on drifts in the northern North Atlantic, *Paleoceanography*, *9*(6), 917–941, doi:10.1029/94PA01438.

Woodruff, F., and S. Savin (1989), Miocene deep water oceanography, *Paleoceanography*, *4*(1), 87–140, doi:10.1029/PA004i001p00087.

Wright, J. D., and K. G. Miller (1996), Control of North Atlantic deep water circulation by the Greenland-Scotland Ridge, *Paleoceanography*, *11*(2), 157–170, doi:10.1029/95PA03696.

Wright, J. D., K. G. Miller, and R. G. Fairbanks (1991), Evolution of modern deep water circulation: Evidence from the late Miocene Southern Ocean, *Paleoceanography*, *6*(2), 275–290, doi:10.1029/90PA02498.

Wright, J. D., K. G. Miller, and R. G. Fairbanks (1992), Early and middle Miocene stable isotopes: Implications for deep water circulation and climate, *Paleoceanography*, *7*(3), 357–389, doi:10.1029/92PA00760.

Yu, J., and H. Elderfield (2008), Mg/Ca in the benthic foraminifera *Cibicidoides wuellerstorfi* and *Cibicidoides mundulus*: Temperature versus carbonate ion saturation saturation, *Earth Planet. Sci. Lett.*, *276*, 129–139, doi:10.1016/j.epsl.2008.09.015.

Zachos, J. C., and L. R. Kump (2005), Carbon cycle feedbacks and the initiation of Antarctic glaciation in the earliest Oligocene, *Global Planet. Change*, *47*(1), 51–66, doi:10.1016/j.gloplacha.2005.01.001.

Zachos, J. C., J. R. Breza, and W. Wise (1992), Early Oligocene ice-sheet expansion on Antarctica: Stable isotope and sedimentological evidence from the Kerguelen Plateau, southern Indian Ocean, *Geology*, *20*(6), 569–573, doi:10.1130/0091-7613(1992)020<0569:EOISEO>2.3.CO;2.

Zachos, J. C., L. D. Stott, and K. C. Lohmann (1994), Evolution of early Cenozoic marine temperatures, *Paleoceanography*, *9*(2), 353–387, doi:10.1029/93PA03266.

Zachos, J. C., T. M. Quinn, and K. A. Salamy (1996), High-resolution (10^4 years) deep-sea foraminiferal stable isotope records of the Eocene-Oligocene climate transition, *Paleoceanography*, *11*(3), 251–266, doi:10.1029/96PA00571.

Zachos, J., M. Pagani, L. Sloan, E. Thomas, and K. Billups (2001), Trends, rhythms, and aberrations in global climate 65 Ma to present, *Science*, *292*, 686–693, doi:10.1126/science.1059412.

Zachos, J. C., et al. (2004), *Early Cenozoic Extreme Climates: The Walvis Ridge Transect*, *Proc. Ocean Drill. Program, Initial Rep.*, vol. 208, edited by H. Nevill, Ocean Drill. Program, College Station, Tex., doi:10.2973/odp.proc.ir.208.2004.

K. G. Miller, Department of Earth and Planetary Sciences, Rutgers University, Wright Geological Laboratory, 610 Taylor Rd., Piscataway, NJ 08854, USA.

A. E. Pusz and R. C. Thunell, Department of Earth and Ocean Sciences, University of South Carolina, 701 Sumter St., Columbia, SC 29208, USA. (apusz@geol.sc.edu)